Experimental and *in silico* investigations of the conformational landscapes of intrinsically disordered proteins : applying geometric approaches at various scales

Thérèse E Malliavin

March 17, 2025, BHSS Taipei, Taiwan

Novel Computational Approaches
for Determining Protein Structures and Dynamics

International Symposium
on Grids & Clouds (ISGC) 2026

UNIVERSITÉ DE LORRAINE

Laboratoire Physique et Chimie Théoriques

cnrs Centre National de la Recherche Scientifique

Laboratoire de Physique et Chimie Théoriques
CNRS UMR 7019, Université de Lorraine, France

ANR-MoST PRCI multiBioStruct

Multi-scale and multi-resolution bio-molecular structure determination by geometric approaches – multiBioStruct (2019-2024)

anr.fr/Project-ANR-19-CE45-0019

- Help of the ANR 361,799 euros
- Duration of the scientific project: 48 Months
- 21 publications recorded in HAL

Antonio Mucherino
IRISA

Simon Hengeveld IRISA (PhD: 2020-2024)

Leo Liberti
LIX, CNRS

Thérèse Malliavin
UL, CNRS

Sammy Khalife
John Hopkins University
(2020-2021)

Wagner da Rocha
LIX (2023-2024)

Jung-Hsin Lin
Academia Sinica
Research Center for Applied Sciences

Chi-Fon Chang
Academia Sinica

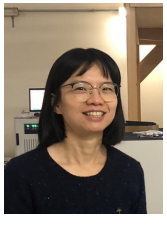

ShuYu Huang
Academia Sinica

Daniel Förster
Université d'Orléans
(2022)

Marina Botnari
LPCT/LUE
(PhD : 2024-)

IRP ExpGeomPro

APPROACHES FOR THE GEOMETRIC EXPLORATION OF THE PROTEIN CONFORMATIONAL SPACE (EXPGEOMPRO)

CNRS-NSTC International Research Project (IRP)

APPROCHES POUR L'EXPLORATION GÉOMÉTRIQUE DE L'ESPACE CONFORMATIONNEL DES PROTÉINES

Thérèse E Malliavin, Laboratoire de Physique et Chimie Théorique, Lorraine University
Keywords: Structural bioinformatics; Calculation of protein structures therese.malliavin@univ-lorraine.fr
Antonio Mucherino, Institut de Recherche en Informatique et Systèmes Aléatoires, University of Rennes.
Keywords: Algorithmics; Optimization; Distance Geometry antonio.mucherino@irisa.fr
Jung-Hsin Lin, Professor, Research Center for Applied Sciences, Academia Sinica, Taiwan.
Keywords: Structural bioinformatics; Computer-aided drug design; Flexible docking problem; Nuclear Magnetic Resonance jhlin@gate.sinica.edu.tw

Exploration of the conformation space for IDPs

Small EDRK-rich factor 1 (SERF1a) Huang et al, AOS Omega, 2026

Promyelocytic leukemia protein (PML)

Exploration of the conformations of IDRs

Reconstruction of protein loops

Ad-hoc solvers for local optimization

Protein structure prediction from local information

Protein conformation from local geometry da Rocha et al, JCIM 2024

Prediction of ω torsion angles

www.gesp.cnrs.fr

2024-2028

Distance Geometry for enumerating proteins conformations

TAiBP protocol for calculating IDP conformations

A. interval Branch-and-Prune (iBP) runs

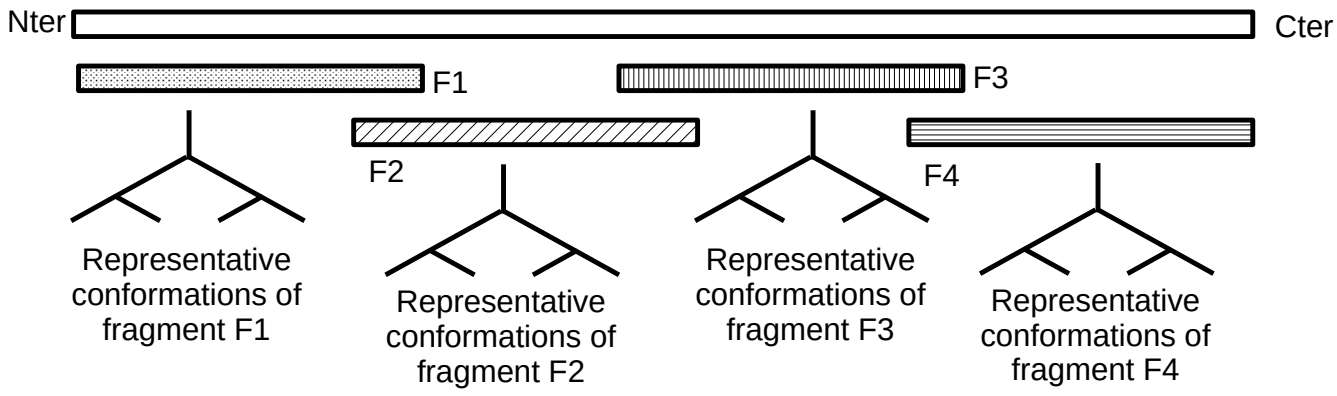

B. Assembly of fragments

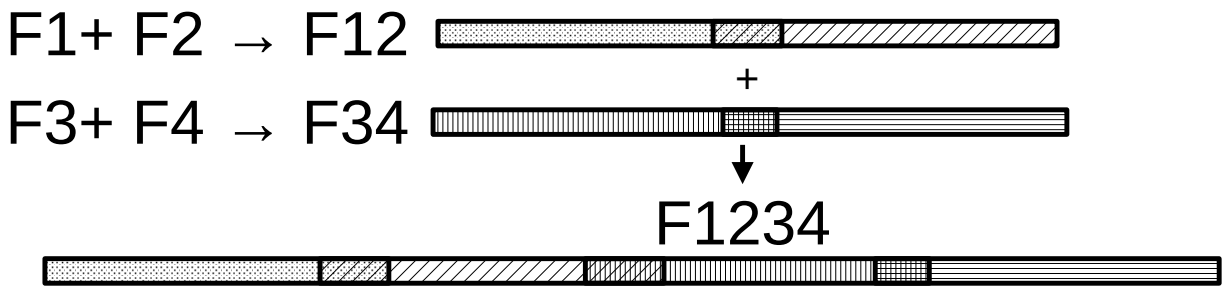

Huang SY, Shih O, Jeng US, Chang CF, Lin JH, **Malliavin TE**. pH sensitivity of the SERF1a conformational ensemble. ACS Omega. 2026

da Rocha W, Liberti L, Mucherino A, **Malliavin TE**. Influence of Stereochemistry in a Local Approach for Calculating Protein Conformations. J Chem Inf Model. 2024

Förster D, Idier J, Liberti L, Mucherino A, Lin JH, **Malliavin TE**. Low-resolution description of the conformational space for intrinsically disordered proteins. Sci Rep. 2022

Malliavin TE. Tandem domain structure determination based on a systematic enumeration of conformations. Sci Rep. 2021

Malliavin TE, Mucherino A, Lavor C, Liberti L. Systematic Exploration of Protein Conformational Space Using a Distance Geometry Approach. J Chem Inf Model. 2019

TAiBP protocol for calculating IDP conformations

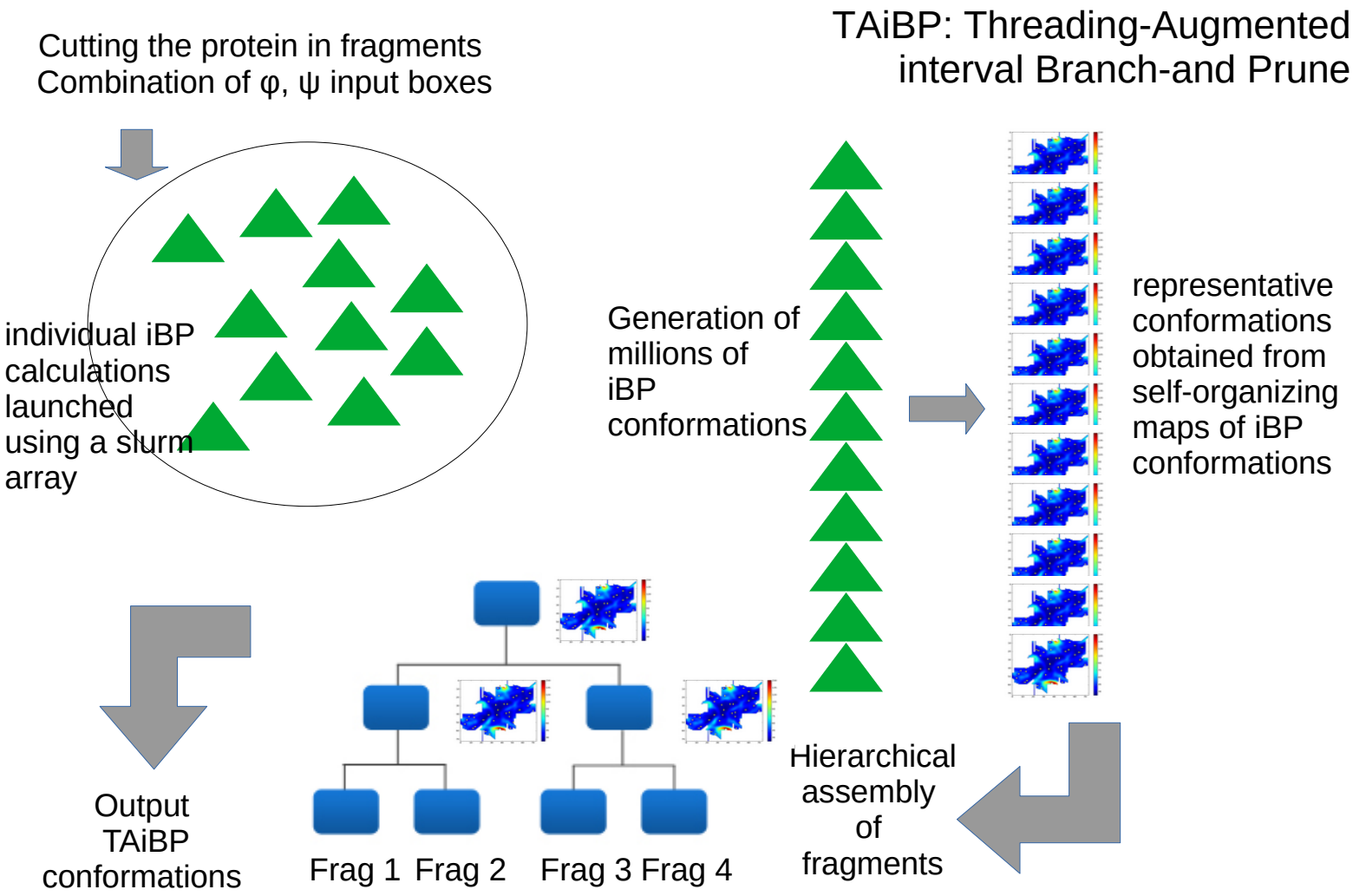

SERF1a disordered protein

Modifier of Aggregation-4/Small EDRK-rich Factor (MOAG4/SERF)

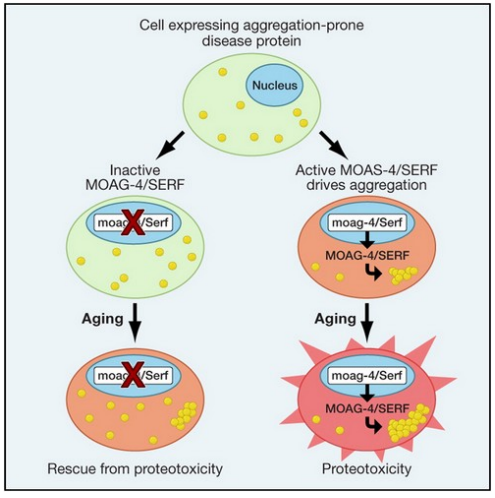

Van Ham et al, Cell 2010

Family of proteins being positive regulator of aggregate formation :

→ for polyglutamine diseases
→ for amyloid-beta
→ for alpha-synuclein

SERF1a binds directly to RNA and improves RNA duplex formation

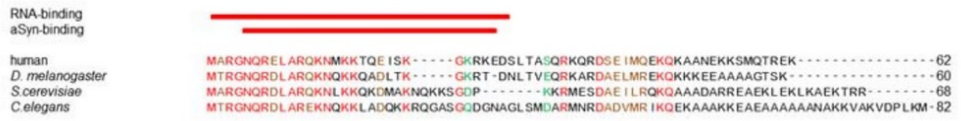

A nucleolus is the part of a eukaryotic cell where ribosomes are made. Seen under a microscope, the nucleolus is a dark spot inside the cell's nucleus. It is made up of dense RNA and proteins

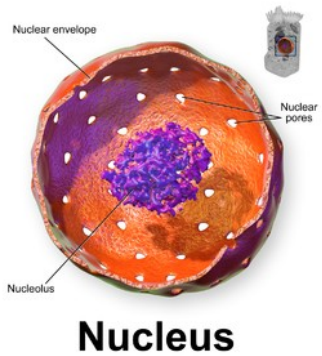

eGFP-SERF1a

RNA-binding defective SERF1a mutant eGFP-K17E

control

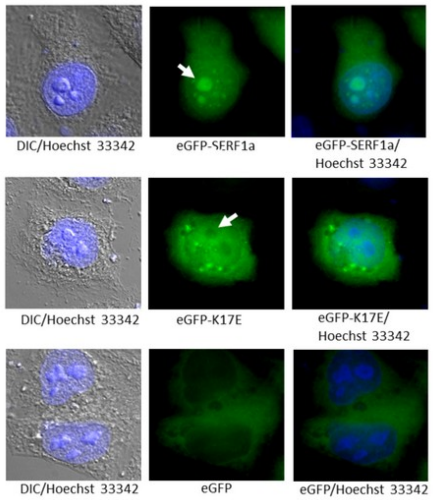

Collab. JH Lin, S Huang and C-F Chang
Academia Sinica, Taiwan

Meyer et al, J Mol Biol 2019

Processing NMR chemical shifts into ϕ,ψ boxes

δ2D predictions

δ2D-v 2.1.0 Camilloni, De Simone, Vranken, Vendruscolo. Biochemistry 51:2224 (2012)

δ2D	Hollingsworth regions
H (Helix)	A, D
E (Extended Beta)	Z, g, B, e
C (Coil)	E, d, G
PPII (Polyproline II)	P

```
PPP PBP ADP BPA ADD ADd BPP DBB PAA BPB PBB BBP AAD BBB AAA EPd PdE dEG EdG dPE
EDd dED EdB dBE EdP dEB PEd EBd GdE BEd DEd DdE BdE EdD dGE EGd dDE GEd dEP EEd
dEE EdE Pdd ddD Bdd ddG ddB dDd dBd Ddd dPd Gdd dGd ddP Edd ddE dEd ddd EAB BdG
ABE eEB PDE BEe EeB DEB BDE dAE eEd EBA Eed EBD EdA deE eEP BeE PeE BAE DEP EAP
EDP EeP AEP Ede AEB PEe EPe BED EBe PAE eBE EPD dEe PED EPA edE AdE EAd PEA DBE
dEA DPE EDB BEA AEd APE ePE PGB dGB GBd GGE EGG GEG PGP dGP BGB PPG GPd BPG dPG
GdP GdB BGP GBB PBG dBG GPB BBG PGd GPP BGd GBP EED DEE EEe EDE EeE eEE AEE EAE
EEA EPG PEG GEB GEP BEG EBG EGB EGP GPE BGE PGE GBE PPd BPd dPP PPB dPB dBP dBB
BdB BBd PBd PdB PdP BdP GEE EEG EGE BBE EBP EBB PBE EPB BEB PEB BPE BEP EPP PPE
PEP EBE EEB BEE PEE EEP EPE EEE
```

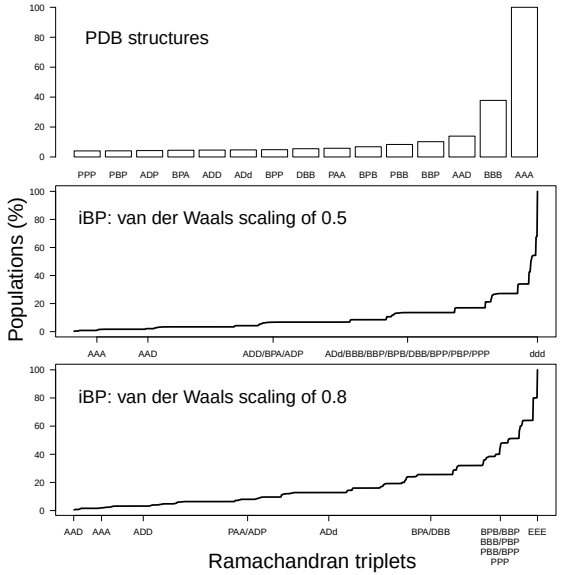

Comparison of δ2D to the probability predictions of TALOS

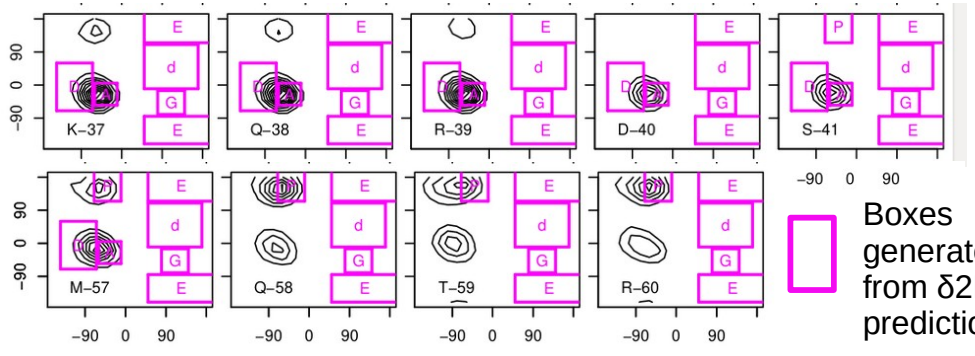

Boxes generated from δ2D predictions

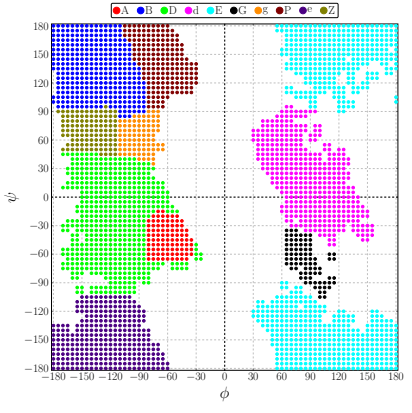

Filtering SERF1a conformations using SAXS curves

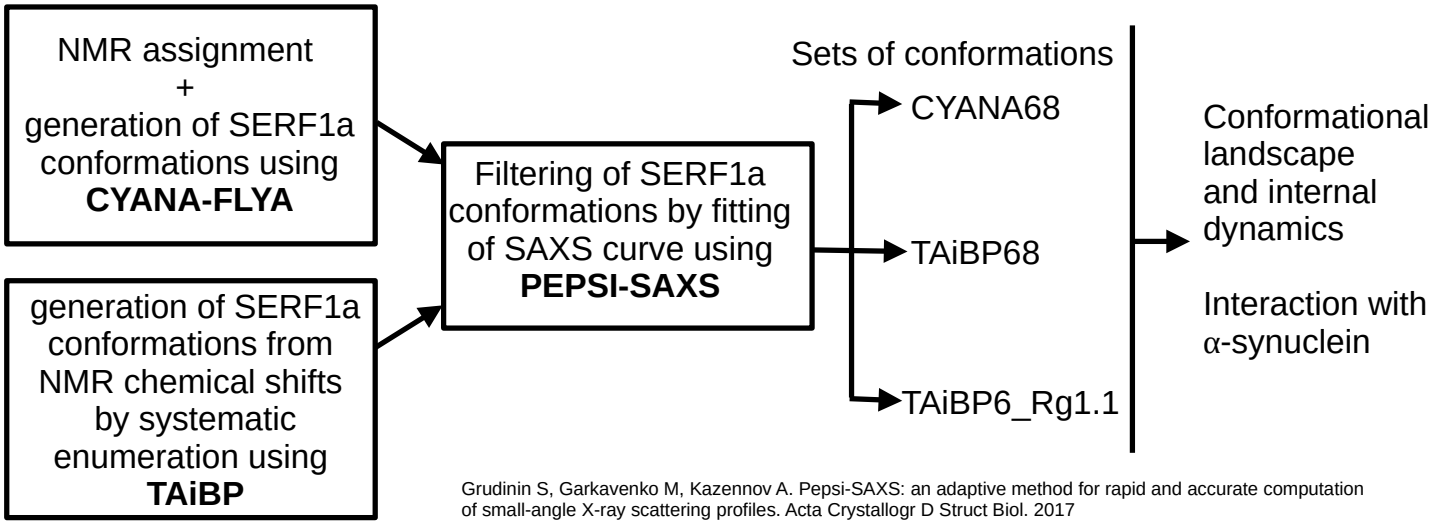

Grudinin S, Garkavenko M, Kazennov A. Pepsi-SAXS: an adaptive method for rapid and accurate computation of small-angle X-ray scattering profiles. Acta Crystallogr D Struct Biol. 2017

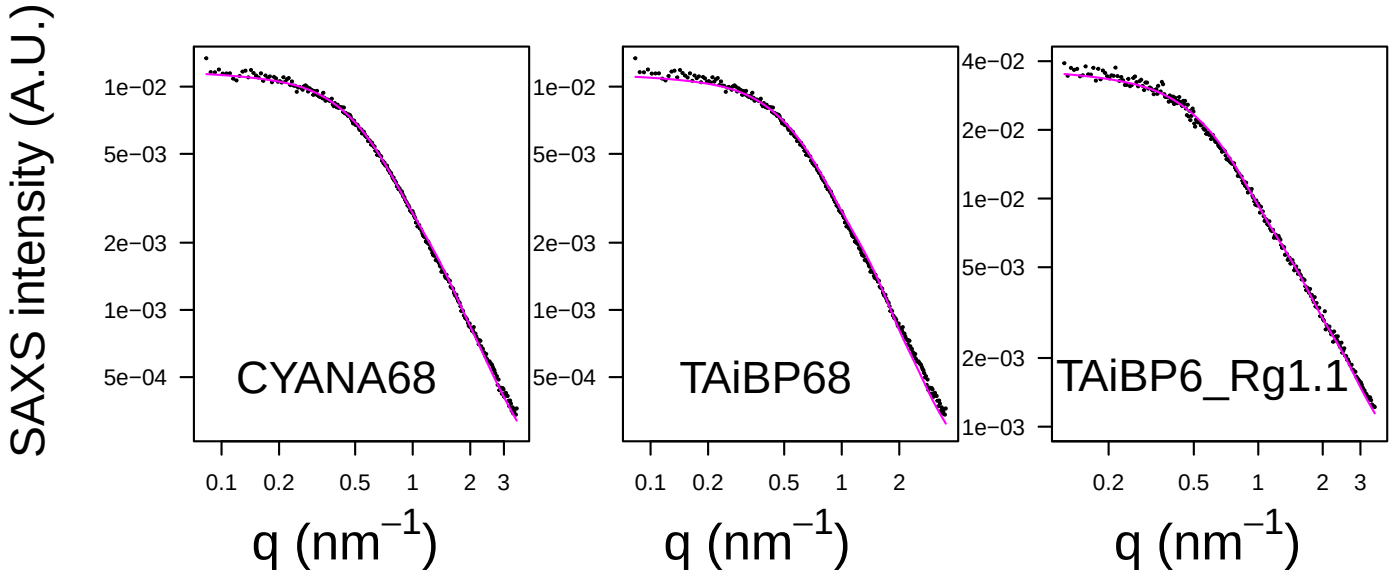

Landscape of SERF1a conformations at pH 6 and 6.8

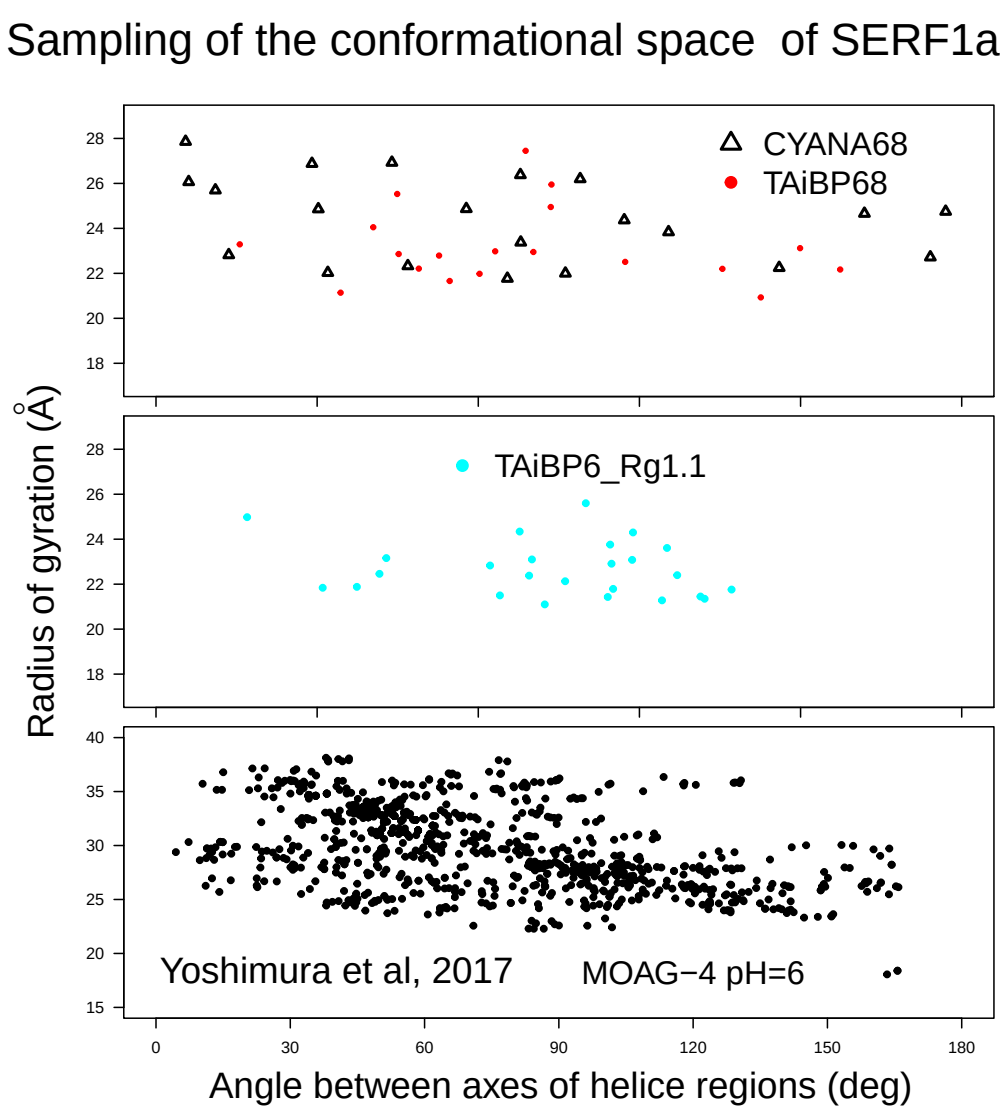

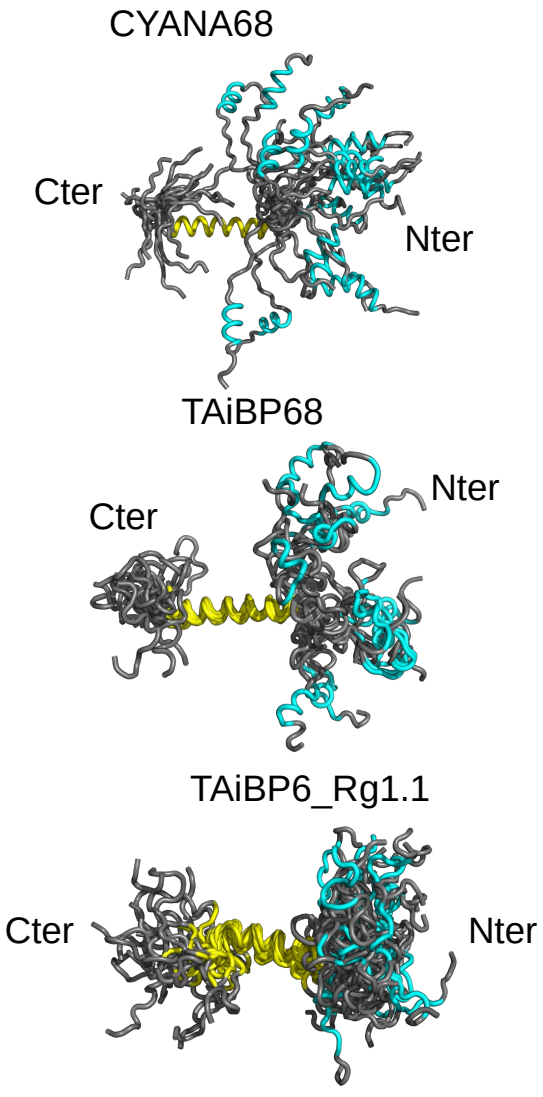

SERF1a internal dynamics

NMR relaxation analysis

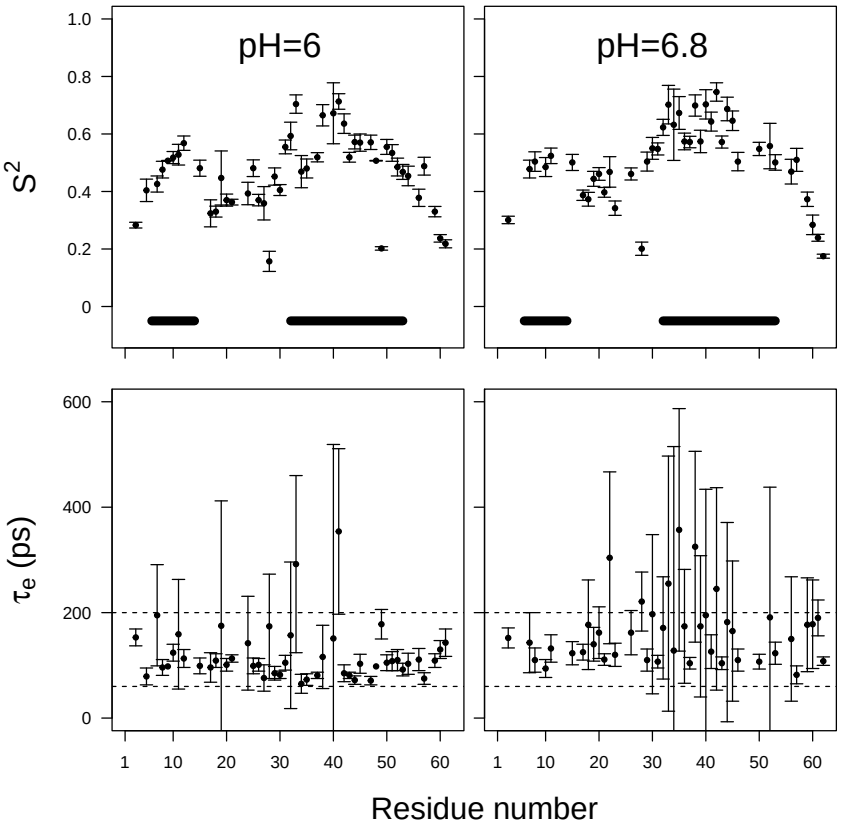

Prediction of order parameter S^2 from SERF1a conformations

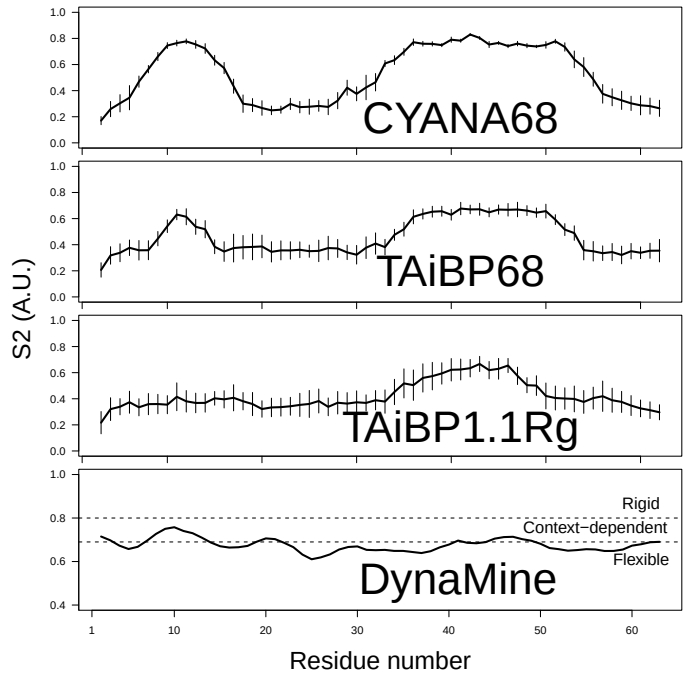

Zhang, F.; Brüschweiler, 2002
Cilia et al, 2013

$$J(\omega) = \frac{2}{5}\tau_m\left[\frac{S^2}{1+(\omega\tau_m)^2} + \frac{(1-S^2)(\tau_e+\tau_m)\tau_e}{(\tau_e+\tau_m)^2+(\omega\tau_e\tau_m)^2}\right]$$

SERF1a inter-molecular interactions

Analysis of possible interaction pockets in the filtered SERF1a conformations

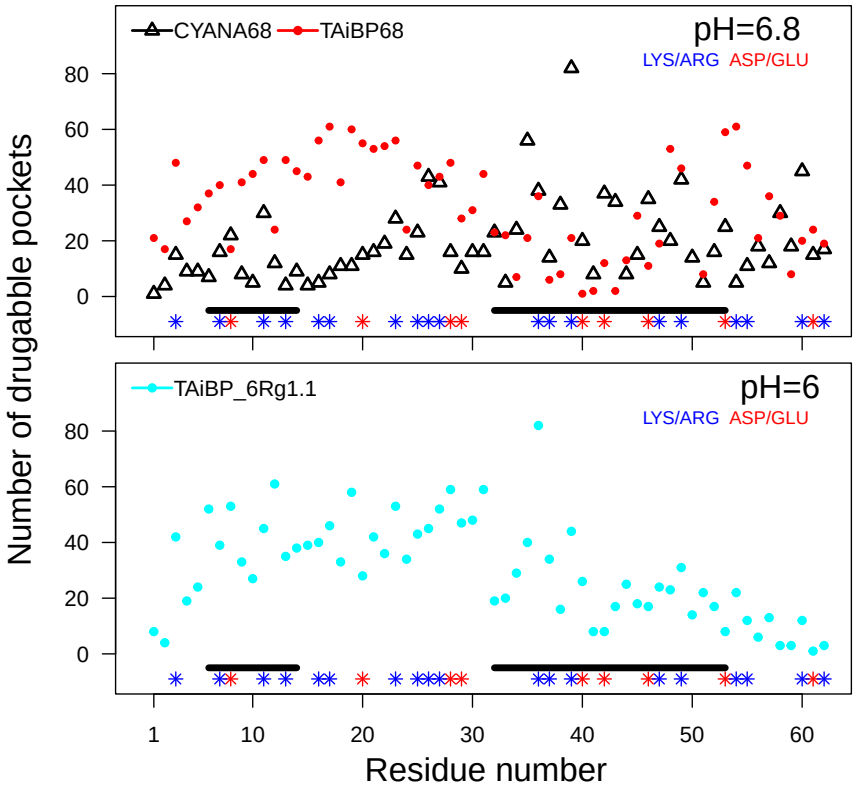

Merle et al. J Mol Biol 2019. Experimental effects of mutations on charged residues of SERF1a

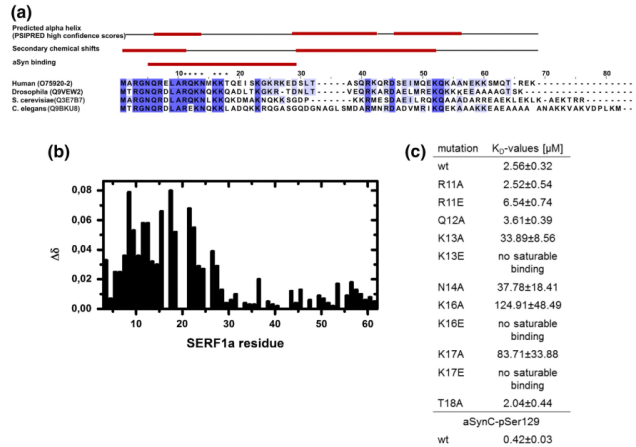

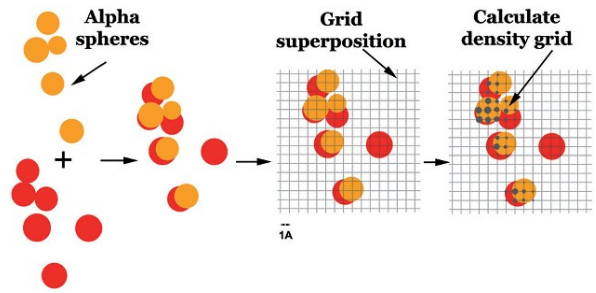

fpocket: online tools for protein ensemble pocket detection and tracking. Schmidtke, Guilloux, Tufféry. NAR 2010

Titration by α-synuclein

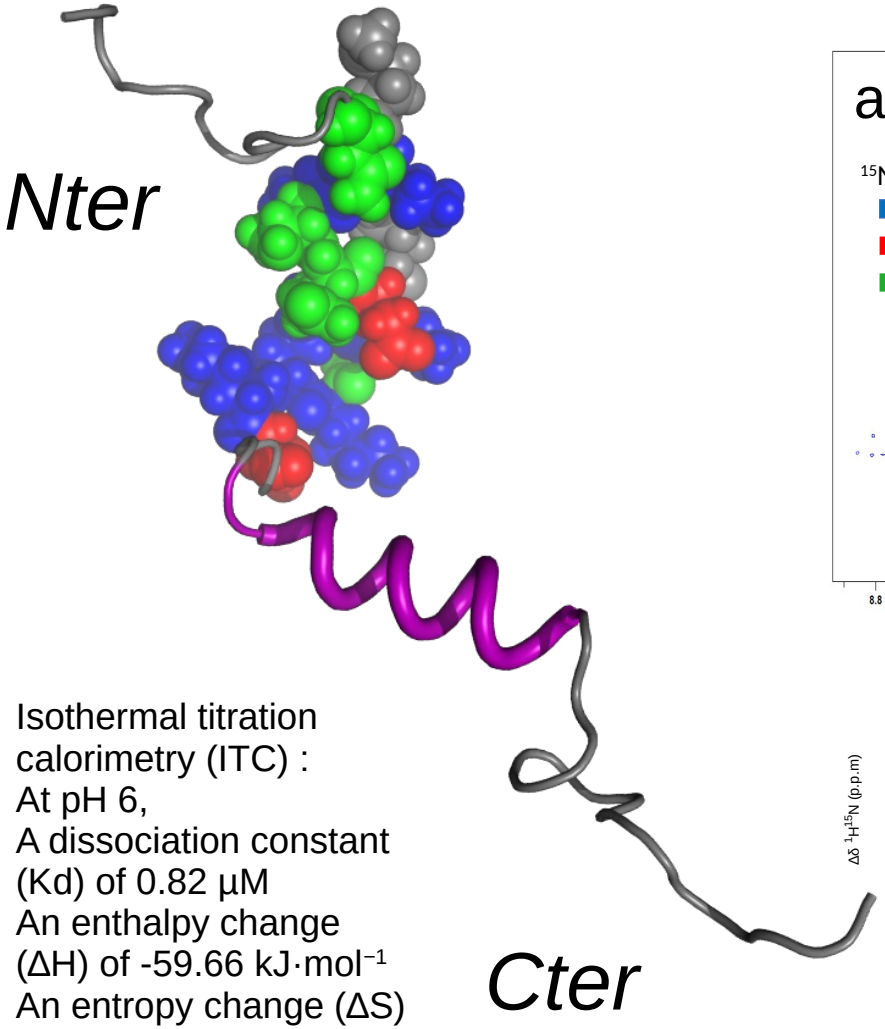

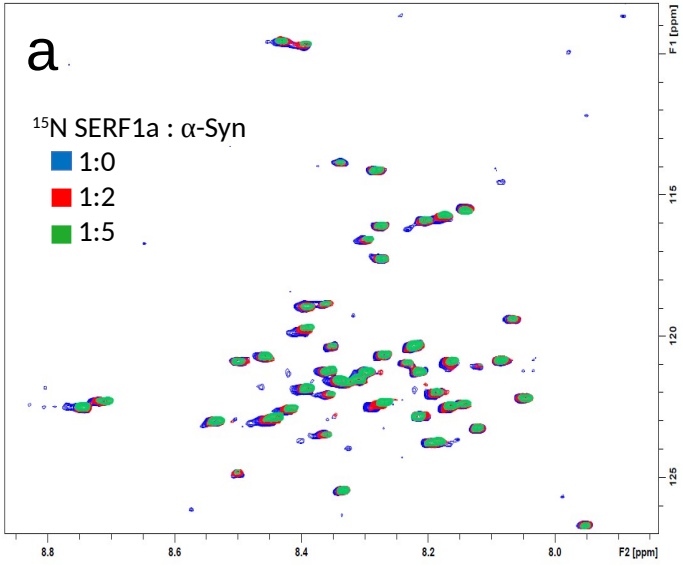

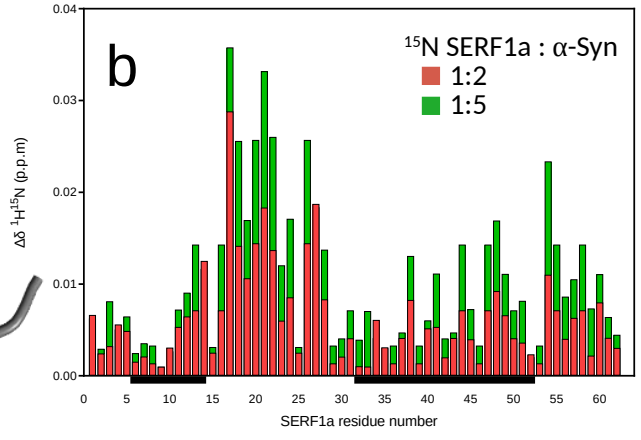

Isothermal titration calorimetry (ITC) :
At pH 6,
A dissociation constant (Kd) of 0.82 µM
An enthalpy change (ΔH) of -59.66 kJ·mol^{-1}
An entropy change (ΔS) of -83.58 J·mol^{-1} ·K^{-1}

SERF1a and condensats

Confocal microscopy images of the EGFP-SERF/α-Syn complex

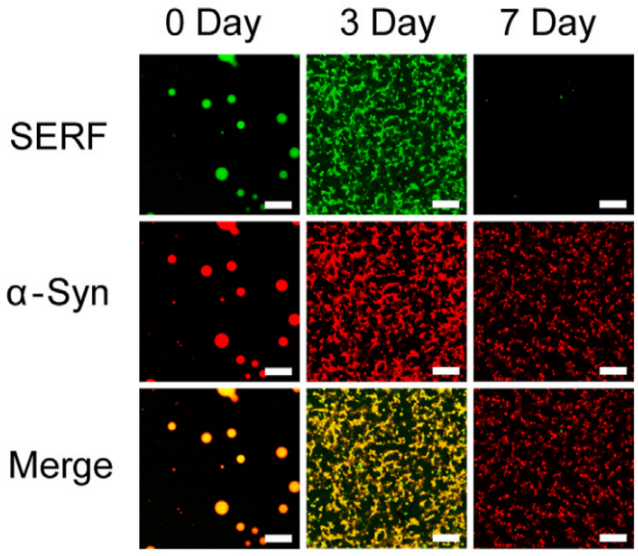

SERF1a/α-Syn cophase separation

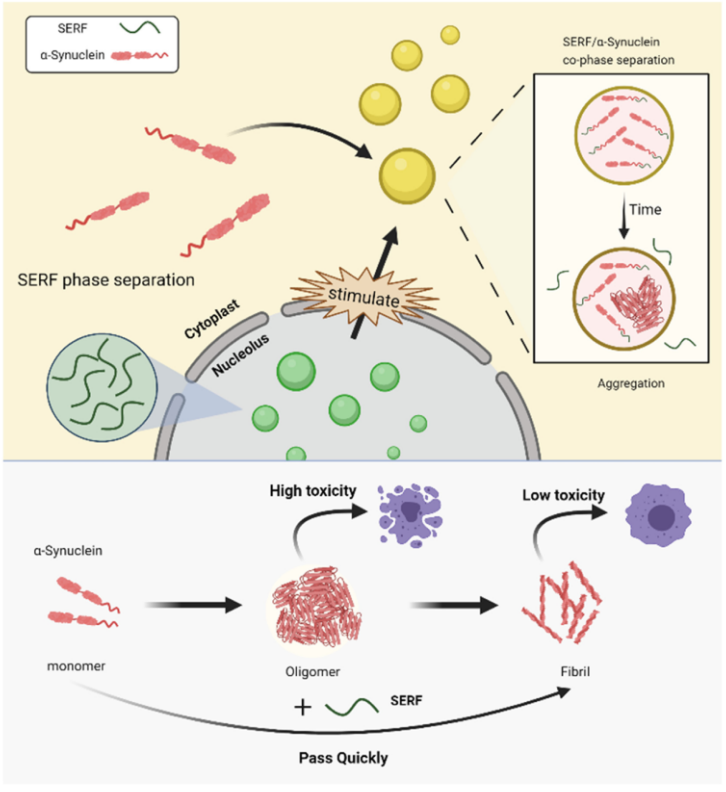

Figure 6. Schematic illustration of the process and function for the SERF/α-Syn cophase separation in the cell.

Liu HN, Wang T, Hu JJ, Chen L, Shi X, Li YM, Luo SZ. The disordered protein SERF promotes α-Synuclein aggregation through liquid-liquid phase separation. J Biol Chem. 2024

SERF1a and electrostatics

Variations of the interactions within the helix

C terminal Helix 2

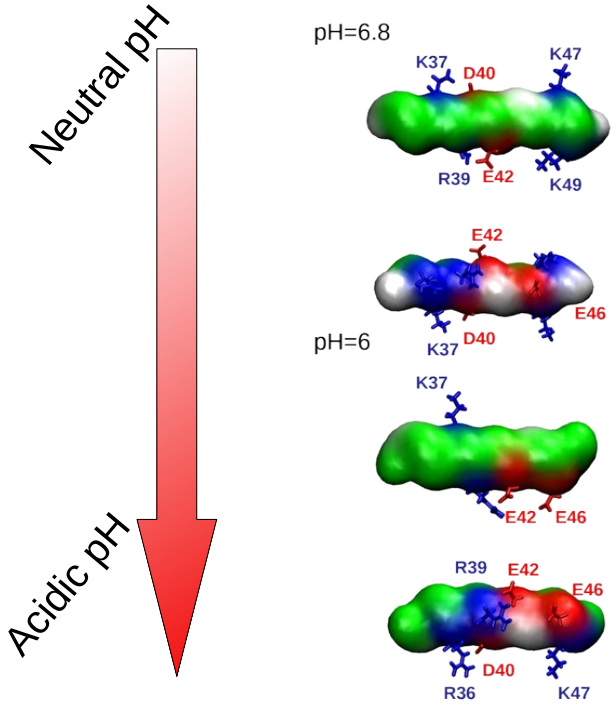

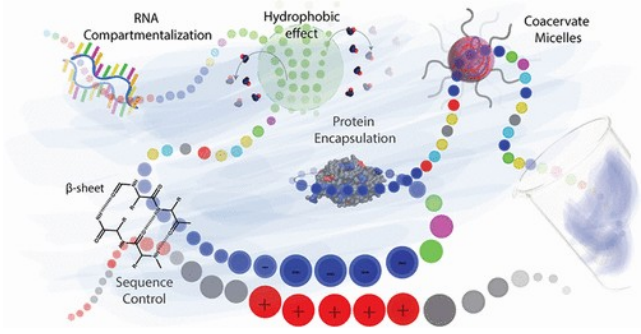

Self-Assembling Polypeptides in Complex Coacervation
Sathyavageeswaran, Sabadini, Perry
Accounts of Chemical Research 2024

Schematic of oppositely charged polymers undergoing complex coacervation and releasing condensed counterions.

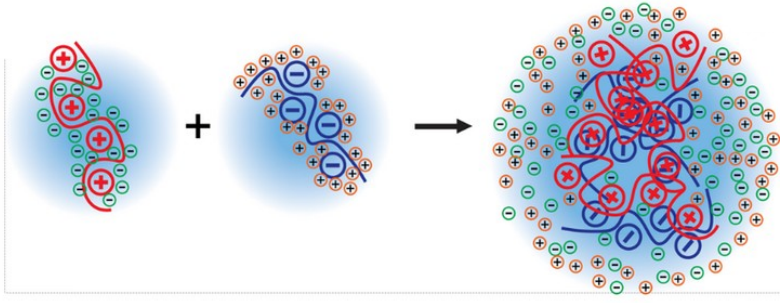

Conclusions

- The Threading-augmented Interval Branch-and-Prune (TAiBP) has generated sets of SERF1a conformations verifying the whole experimental knowledge available protein conformatioal space.
- The TAiBP conformations agree with nternal dynamics measurements.
- The NMR measurements at two pH values along with the analysis of representative conformations provides a model of the SERF1a-αSynuclein interaction.

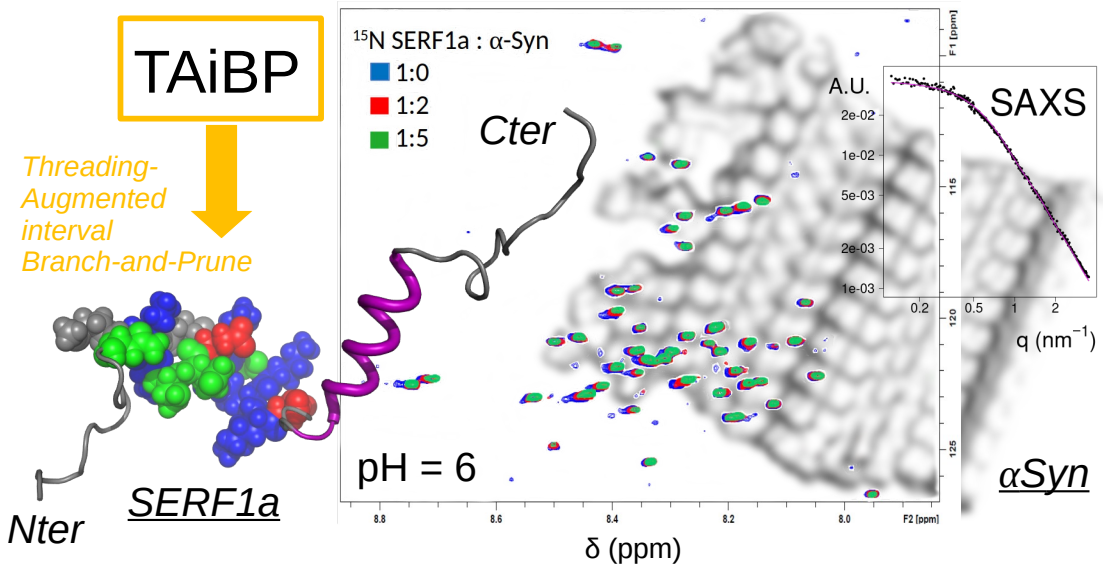

Coarse-graining of proteins from the geometry of secondary structure elements

Coarse-graining of protein structures

Martini

Bottom → Up

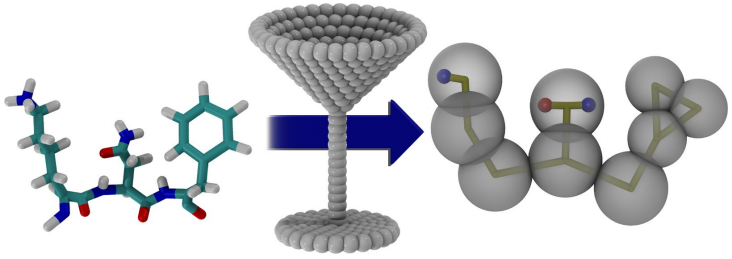

Siewert J Marrink

de Jong DH, Singh G, Bennett WF, Arnarez C, Wassenaar TA, Schäfer LV, Periole X, Tieleman DP, Marrink SJ. Improved Parameters for the Martini Coarse-Grained Protein Force Field. J Chem Theory Comput. 2013 Jan 8;9(1):687-97.

Top → Down (soft shapes)

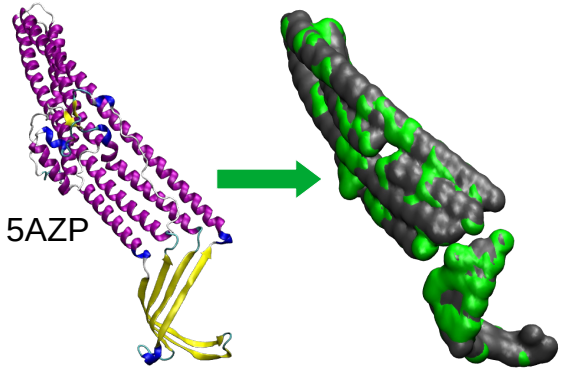

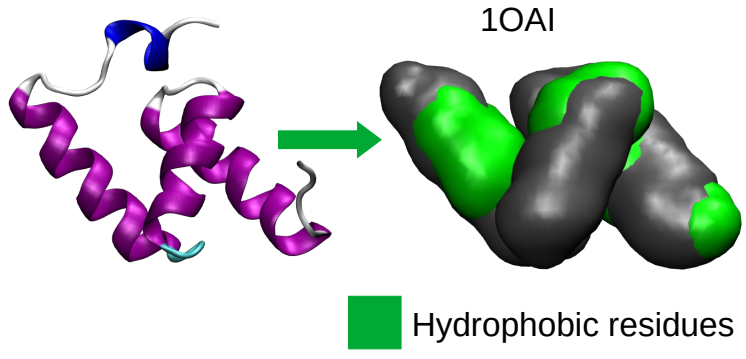

Hydrophobic residues

Membrane proteins

Channel and transporters

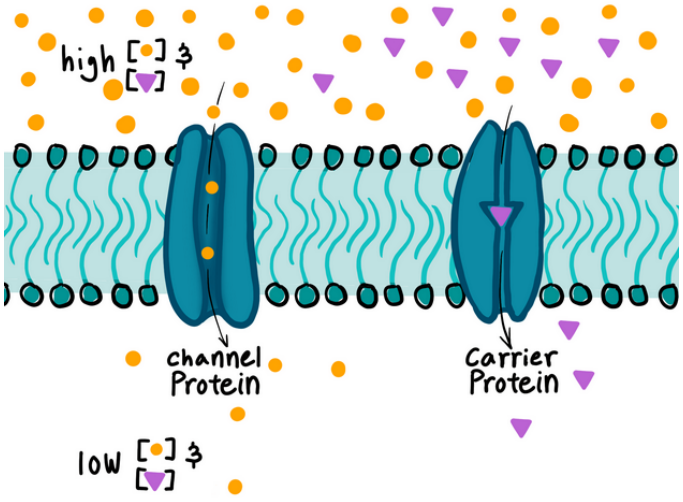

Sylvia Freeman, www.expii.com

Vesicles fusion

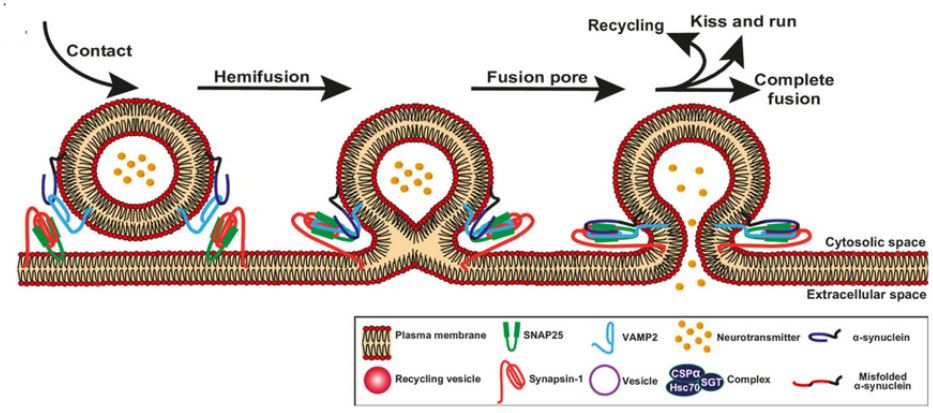

Sarchione et al, Cells 2021

Pore-forming proteins

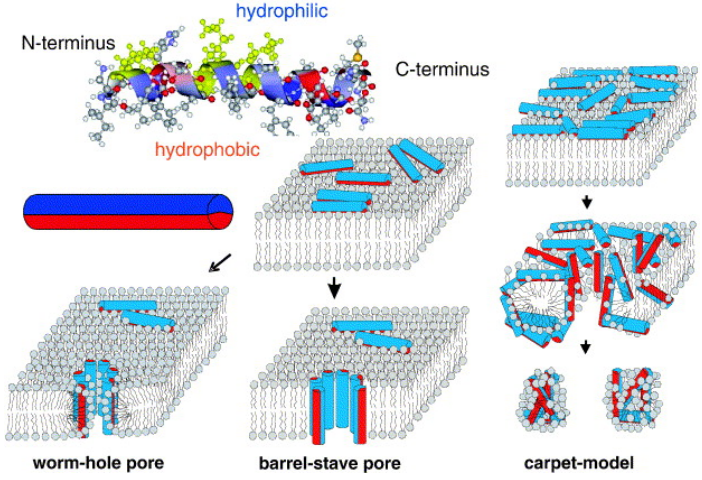

Hong et al, Molecules 2019

- The protein/membrane system is highly flexible
- Respective influence of the two interaction partners
- Sparse structural information
- Complex multi-body system

Pore-forming toxin

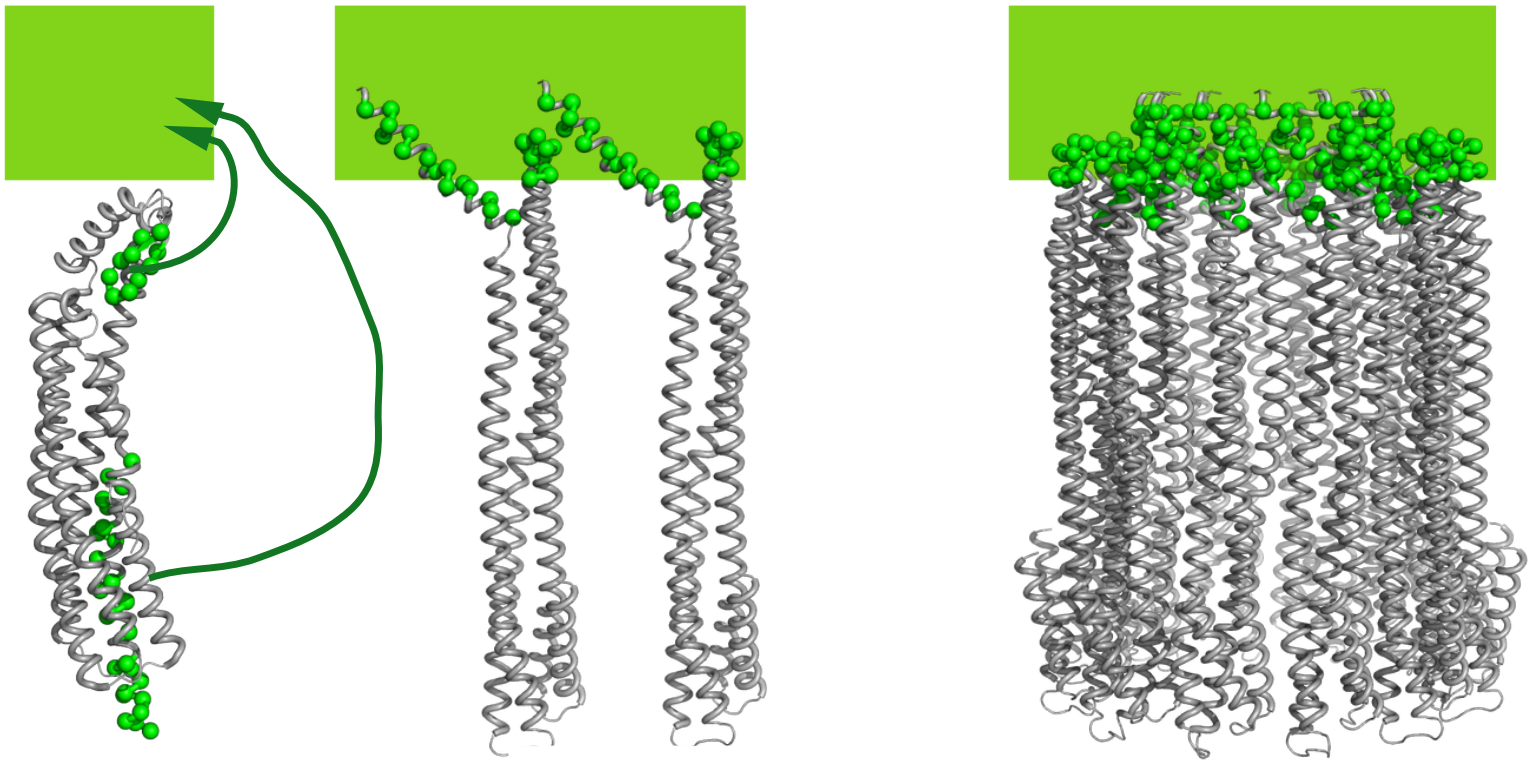

PDB: 1QOY — Cooperativity → PDB: 2WCD

cytolysine A (ClyA) : enteropathogens *Escherichia coli* and *Salmonella* destroy cells by causing their lysis

Coarse-grained model of protein-membrane interaction

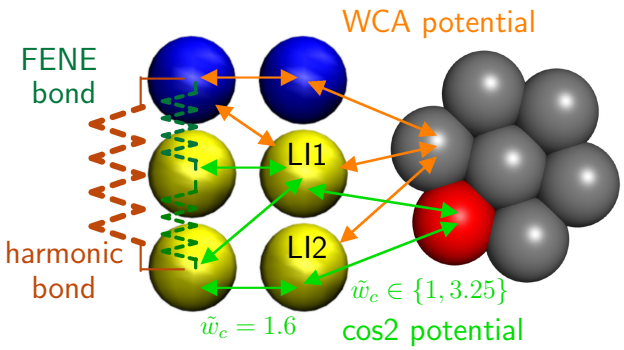

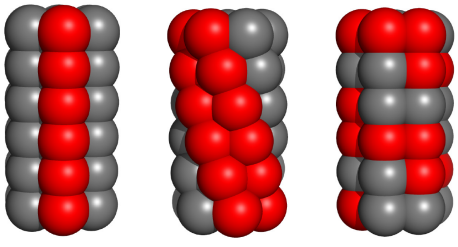

ESPResSO MD

$$V_{\mathrm{WCA}}(r) = \begin{cases} 4\epsilon\left[\left(\frac{b}{r}\right)^{12} - \left(\frac{b}{r}\right)^{6} + \frac{1}{4}\right], & r \le r_{\mathrm{c}} \\ 0, & r > r_{\mathrm{c}} \end{cases}, \qquad (3)$$

where $b = 0.95\sigma$ and $r_{\mathrm{c}} = 2^{1/6}b$.

$$V_{\cos 2}(r) = \begin{cases} 4\epsilon\left[\left(\frac{\sigma}{r}\right)^{12} - \left(\frac{\sigma}{r}\right)^{6}\right], & r < r_{\mathrm{c}} \\ -\epsilon\cos^2\frac{\pi(r - r_{\mathrm{c}})}{2w_{\mathrm{c}}}, & r_{\mathrm{c}} \le r \le r_{\mathrm{c}} + w_{\mathrm{c}} \\ 0, & r > r_{\mathrm{c}} + w_{\mathrm{c}} \end{cases} \qquad (4)$$

$$V_{\mathrm{FENE}}(r) = -\frac{1}{2}k_{\mathrm{FENE}}{r_\infty}^2 \log\left[1 - \left(\frac{r}{r_\infty}\right)^2\right] \qquad (1)$$

$$V_{\mathrm{bend}}(r) = \frac{1}{2}k_{\mathrm{bend}}(r - 4\sigma)^2 \qquad (2)$$

Illya and Deserno, Biophys. J., 2008, 95, 4163–4173.
Cooke and Deserno, J. Chem. Phys., 2005, 123, 224710.

Cylinder modeled with a tensegrity structure

Table 1 Equilibrium lengths r_{eq} used to define the cylinder tensegrity (see eqn (6)). The state of the harmonic bond depends on whether r_{eq} is smaller or larger than the geometrical distance r_0 between the beads at the beginning of the simulation. The parameters of the bonds between the peripheral beads of adjacent disks depend on the angle α_0 obtained from eqn (5) with $R_1 = 2r_c \sin\frac{\alpha_0}{2}$, $R_2 = 2r_c \sin\frac{60^\circ - \alpha_0}{2}$, and $R_3 = 2r_c \sin\frac{60^\circ + \alpha_0}{2}$. Note that $R_1 = R_2$ for $\alpha_0 = 30^\circ$

Beads	r_0	r_{eq}	State
Within the same disk	r_c	$1.2r_c$	Compressed
Within adjacent disks			
(1) Center and peripheral	$\sqrt{2}r_c$	$1.2r_c$	Stretched
(2) Center and center	r_c	$1.2r_c$	Compressed
(3) Peripheral and peripheral			
$\alpha_0 \neq 30^\circ$			
1st neighbors	$\sqrt{(r_c)^2+(R_1)^2}$	$1.05\sqrt{(r_c)^2+(R_1)^2}$	Compressed
2nd neighbors	$\sqrt{(r_c)^2+(R_2)^2}$	$0.95\sqrt{(r_c)^2+(R_2)^2}$	Stretched
3rd neighbors	$\sqrt{(r_c)^2+(R_3)^2}$	$0.95\sqrt{(r_c)^2+(R_3)^2}$	Stretched
$\alpha_0 = 30^\circ$			
1st neighbors	$\sqrt{(r_c)^2+(R_1)^2}$	$1.05\sqrt{(r_c)^2+(R_1)^2}$	Compressed
2nd neighbors	$\sqrt{(r_c)^2+(R_3)^2}$	$0.95\sqrt{(r_c)^2+(R_3)^2}$	Stretched

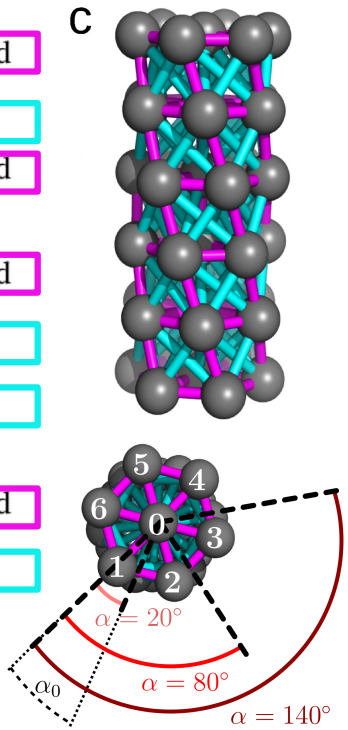

$$V_{cyl}(r) = \frac{1}{2}k_{cyl}(r - r_{eq})^2,$$

where $k_{cyl} = 200\epsilon/\sigma^2 = 778\,\mathrm{pN\,nm^{-1}}$ is the spring constant and r_{eq} is the equilibrium length of the bond.

The tensegrity cylinder is elastic

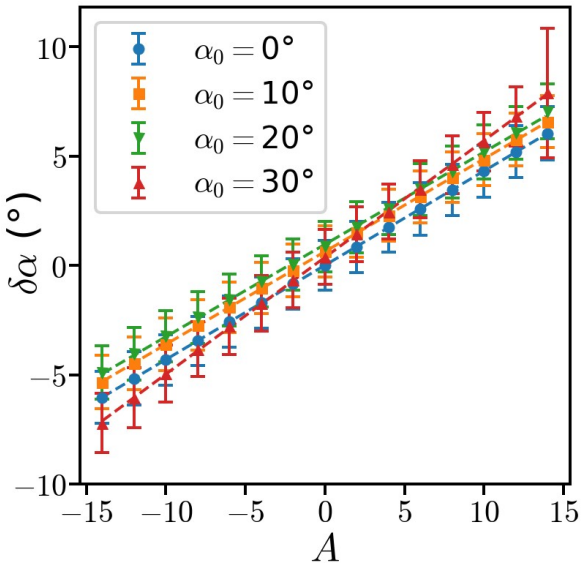

van Reenen et al.
Biophysical J 2013
Janssen et al.
Biophysical J 2011

IgC protein :
experimental
torsional rigidity
ranging from
500 to 5000 pN nm^2

τ_{cyl} = torque

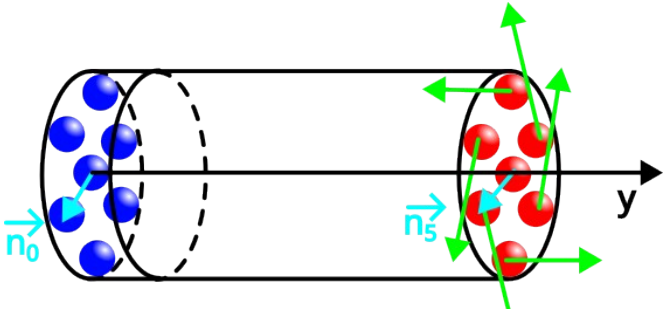

$$\delta\alpha = \frac{\tau_{\mathrm{cyl}} L}{5\chi}$$

Table 2 Torsional rigidity χ and its standard deviation σ_χ obtained from the linear regression of the simulation results of Fig. 2 together with the shift $\delta\alpha$ from the nominal value α_0 for vanishing external torque

α_0 (deg)	χ (pN nm^2)	σ_χ (pN nm^2)	$\delta\alpha$ ($A = 0$) (deg)
0	2939	29	−0.01
10	2980	28	0.77
20	2956	28	0.73
30	2431	25	0.36

Configuration space

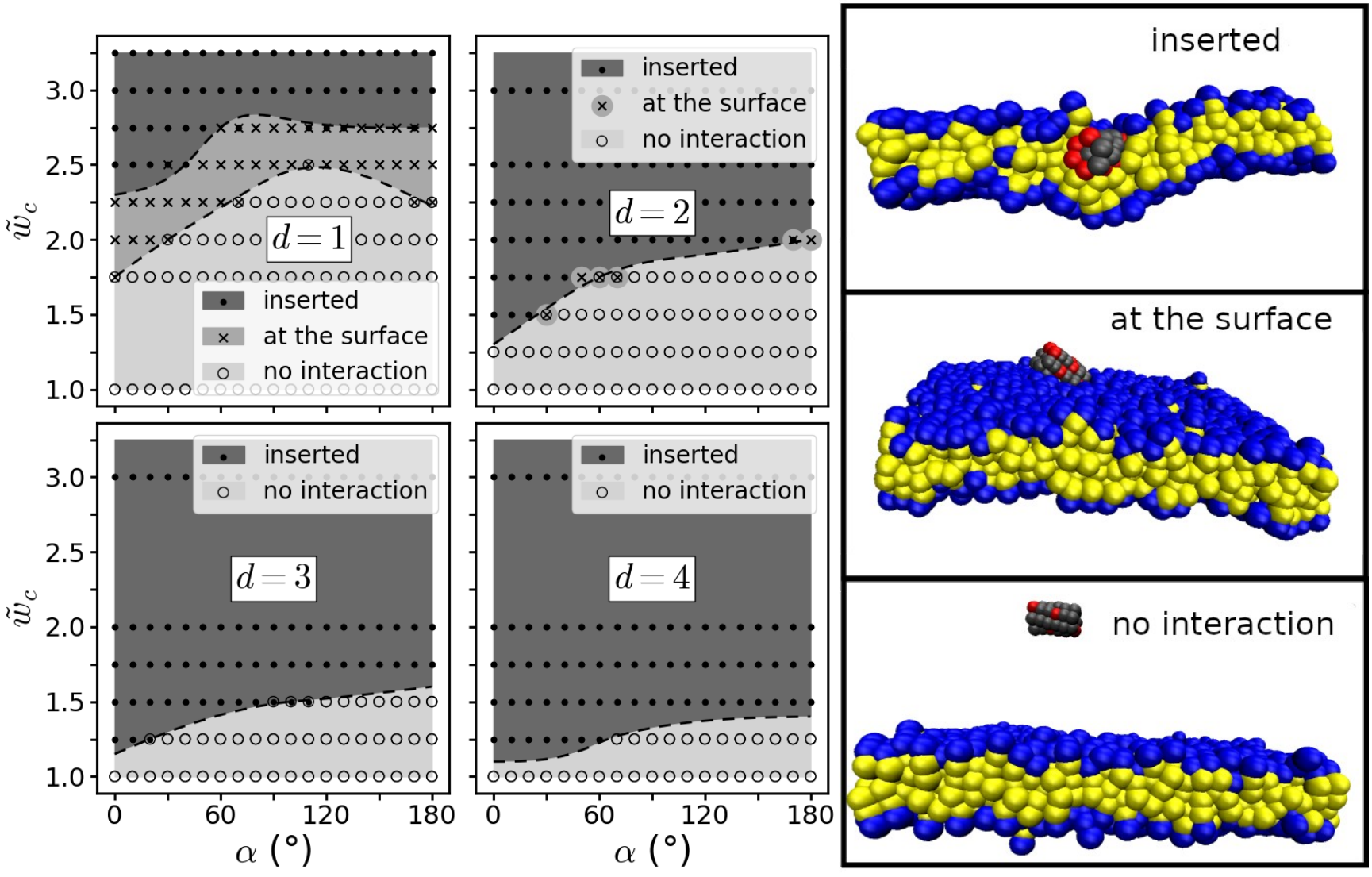

Klein J, Schad L, Malliavin TE, Müller MM. Protein-membrane interactions with a twist. Soft Matter. 2025 Jun 4;21(22):4336-4350. doi: 10.1039/d4sm01494d.

Cylinder orientation in the membrane

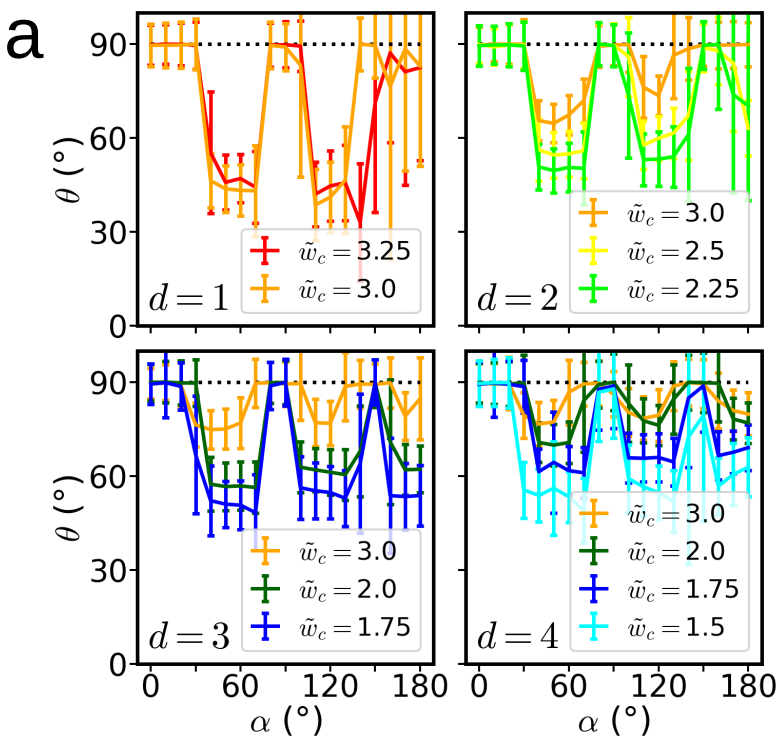

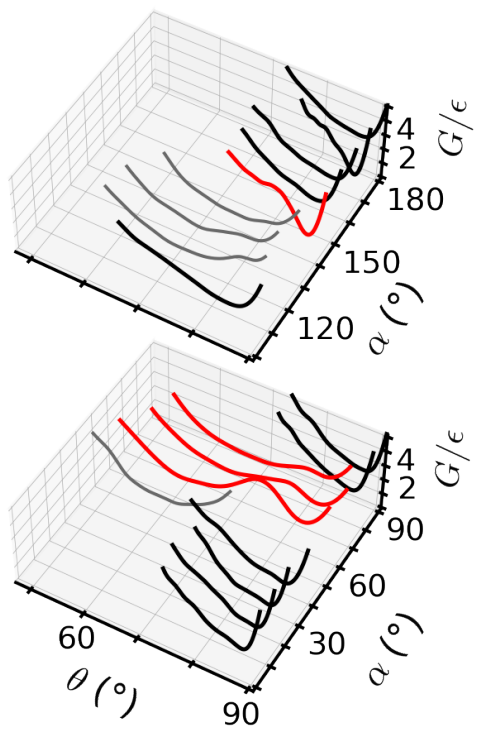

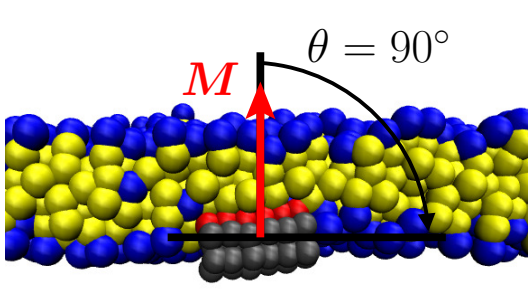

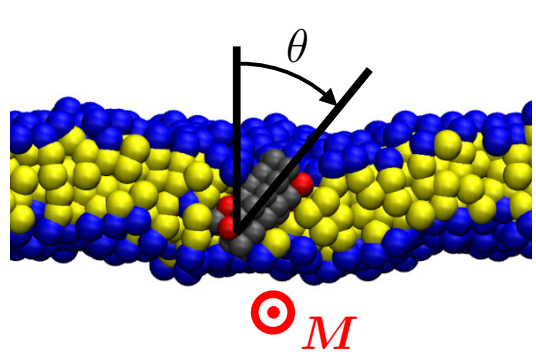

Cylinder orientation is determined by the hydrophic moment

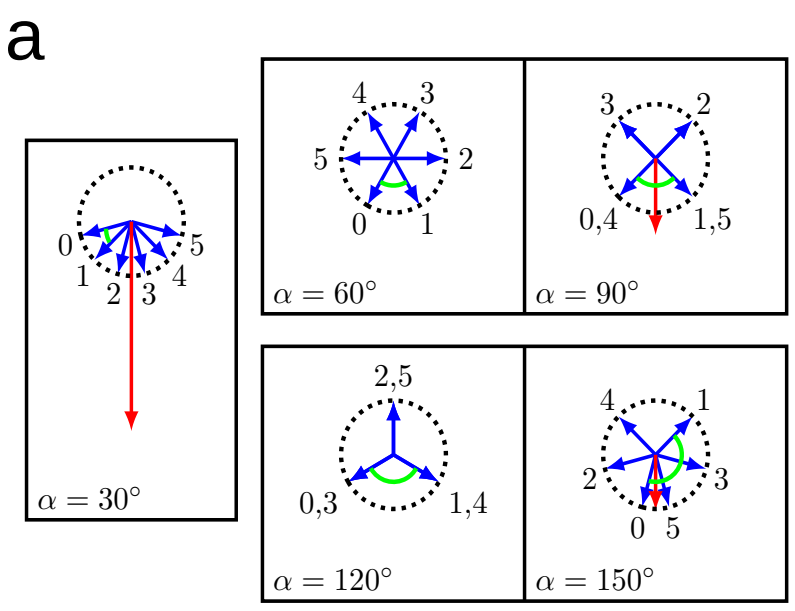

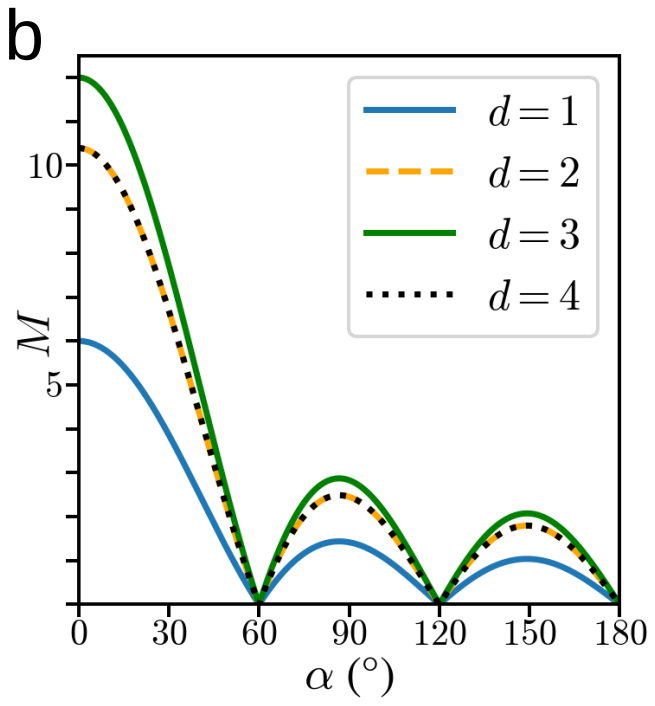

$$\boldsymbol{M} = \sum_i \boldsymbol{M}_i \qquad \boldsymbol{M} = \left(\begin{pmatrix} 1 & 0 \\ 0 & 1 \end{pmatrix} + \sum_{n=1}^{5} \begin{pmatrix} \cos(n\alpha) & -\sin(n\alpha) \\ \sin(n\alpha) & \cos(n\alpha) \end{pmatrix} \right) \begin{pmatrix} \mu \\ 0 \end{pmatrix}$$

$$M = 2\mu \left| \cos\left(\frac{\alpha}{2}\right) + \cos\left(\frac{3\alpha}{2}\right) + \cos\left(\frac{5\alpha}{2}\right) \right|$$

Eisenberg D, McLachlan AD. Solvation energy in protein folding and binding. Nature. 1986 Jan 16-22;319(6050):199-203. doi: 10.1038/319199a0. PMID: 3945310.

The deformation of the membrane is related to cylinder orientation

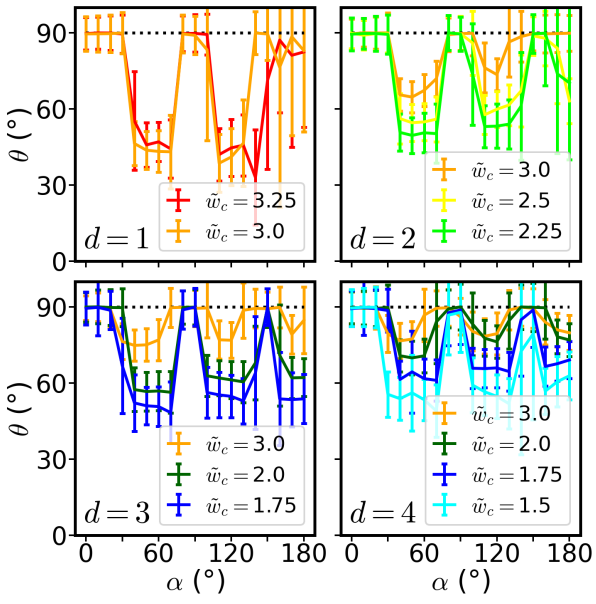

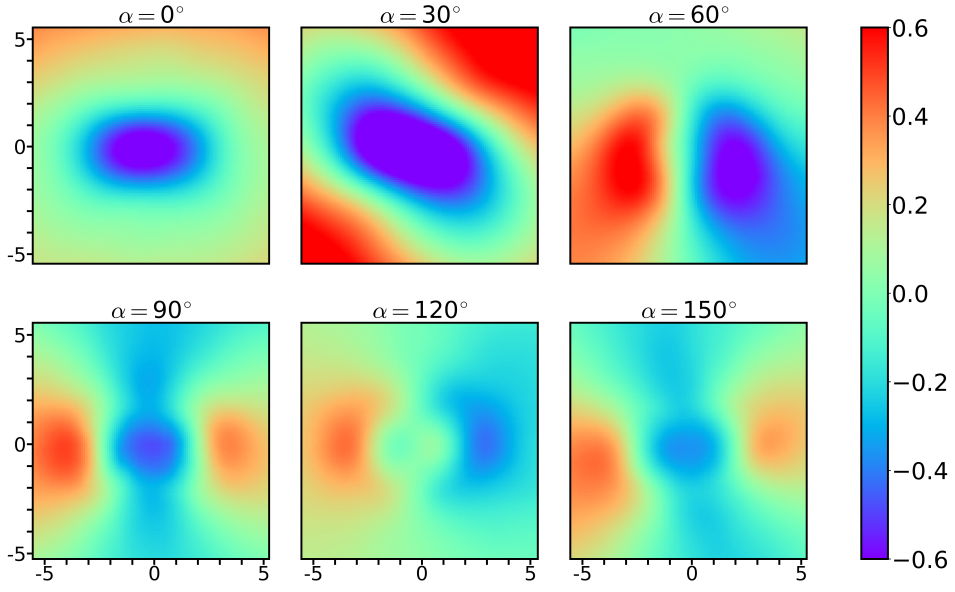

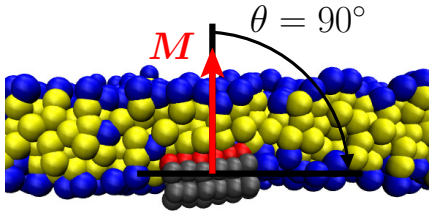

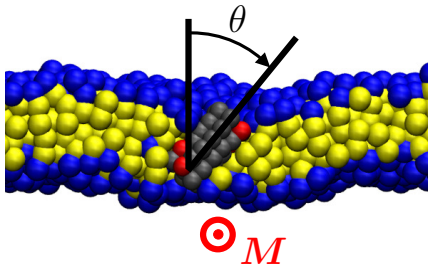

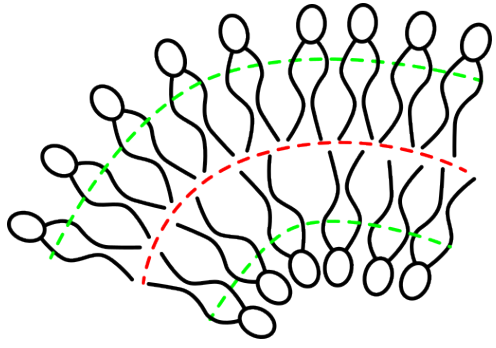

The deformation of the membrane is described by the Twister model

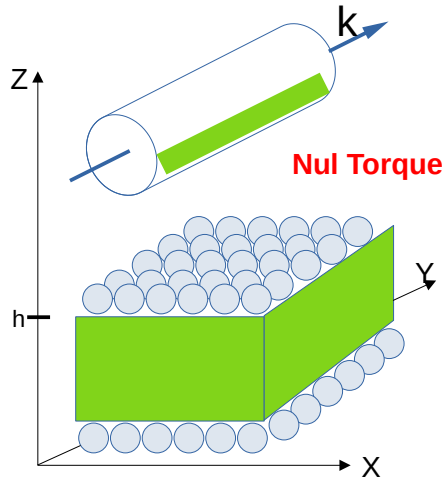

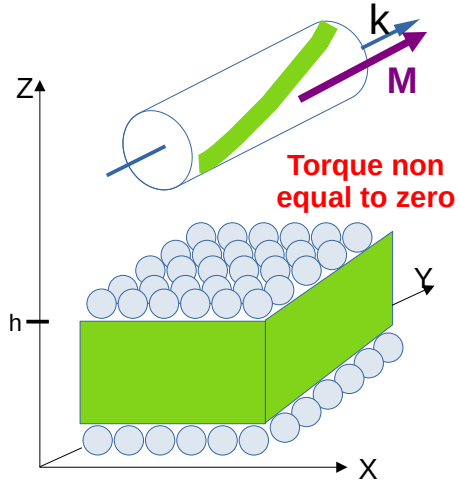

Continuous elastic mode of protein-membrane interaction
=
Energy of the interaction between the torque and the membrane
+
Energy of membrane deformation : Helfrich model

$$E_{\mathrm{mem}} = \int \mathrm{d}A \left(2B_{\mathrm{m}}H^2 + \sigma\right)$$

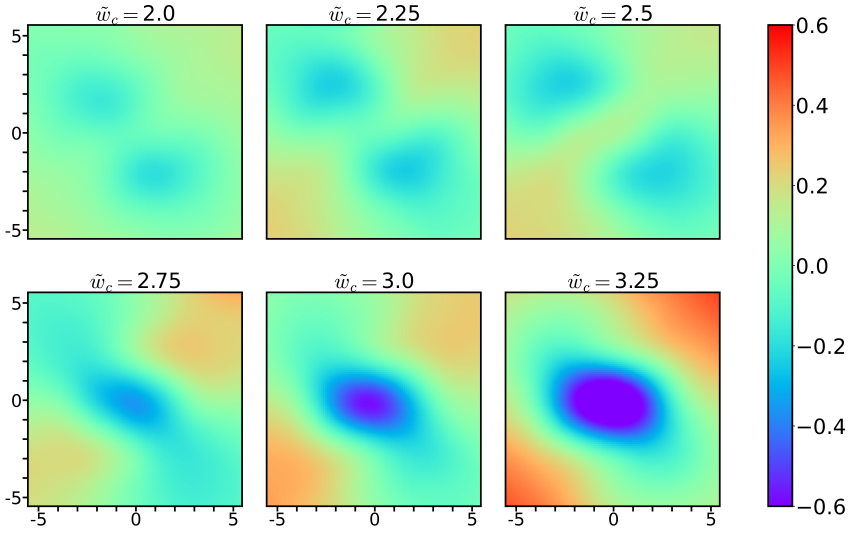

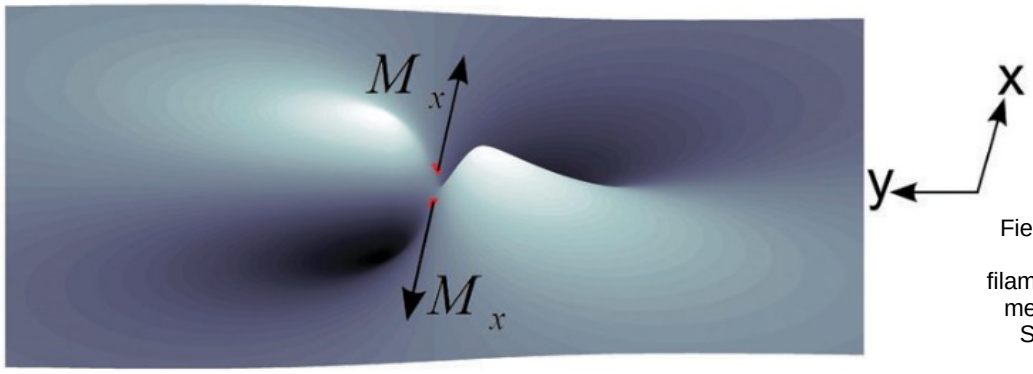

Fierling et al. How bio-filaments twist membranes. Soft Matter 2016

Membrane thinning and thickening

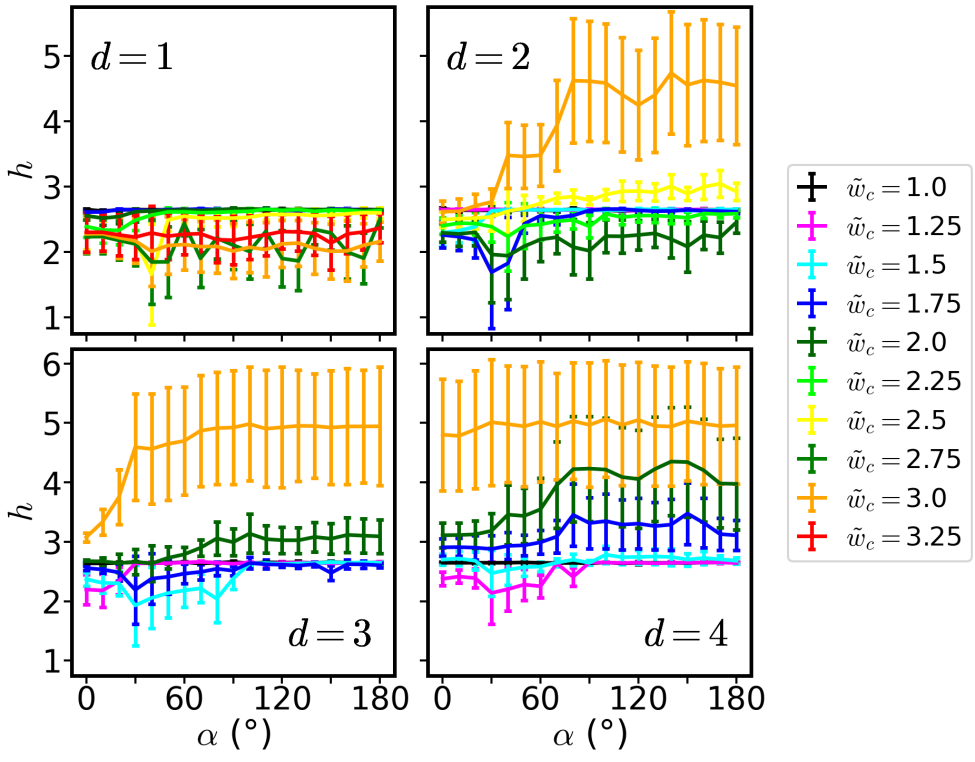

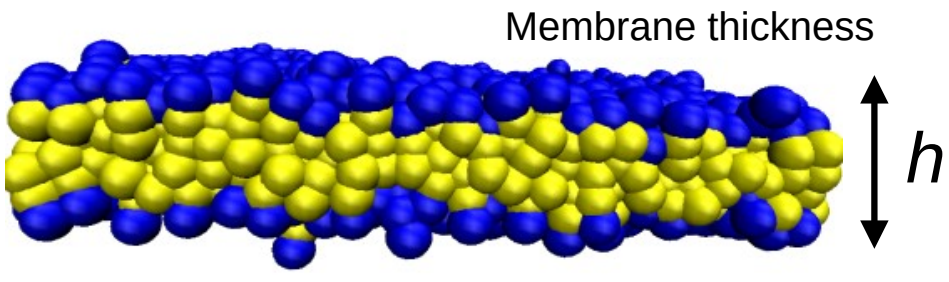

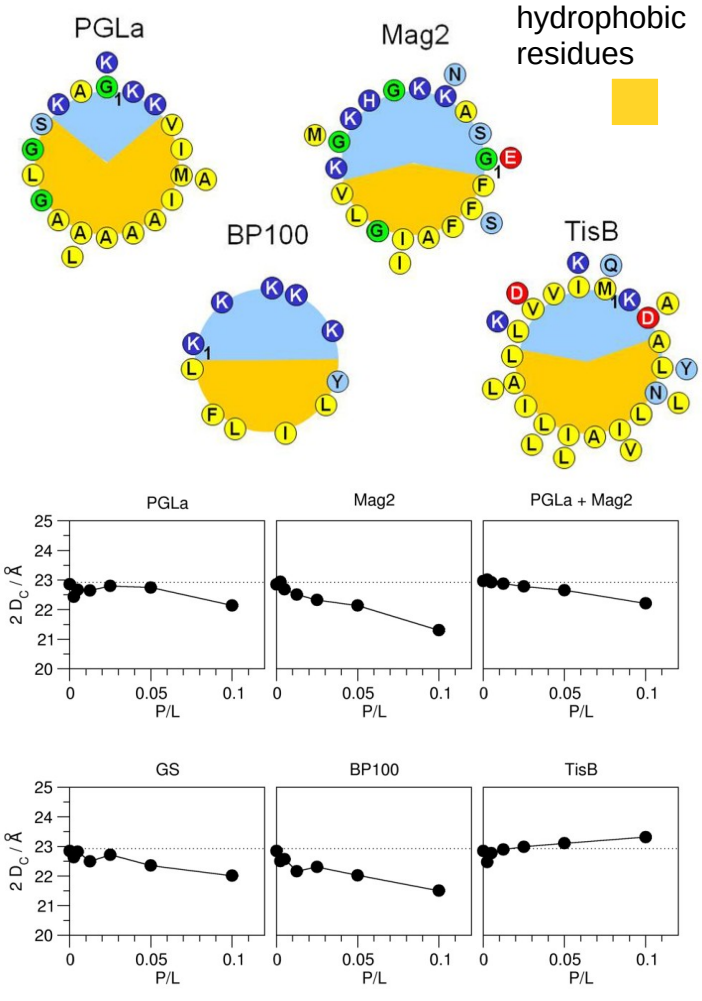

Grage et al. Membrane Thinning and Thickening Induced by Membrane-Active Amphipathic Peptides. Front Cell Devt Biol 2016

Coarse-graining of protein structures

Martini

Bottom → Up

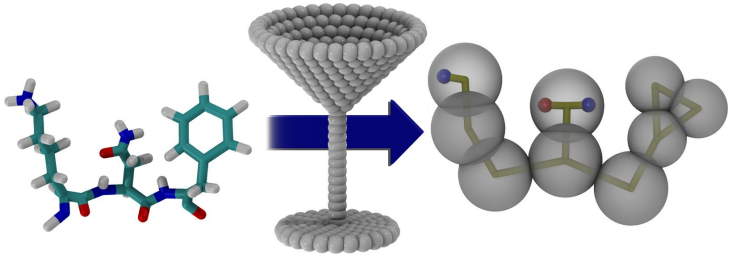

Siewert J Marrink

de Jong DH, Singh G, Bennett WF, Arnarez C, Wassenaar TA, Schäfer LV, Periole X, Tieleman DP, Marrink SJ. Improved Parameters for the Martini Coarse-Grained Protein Force Field. J Chem Theory Comput. 2013 Jan 8;9(1):687-97.

Top → Down (soft shapes)

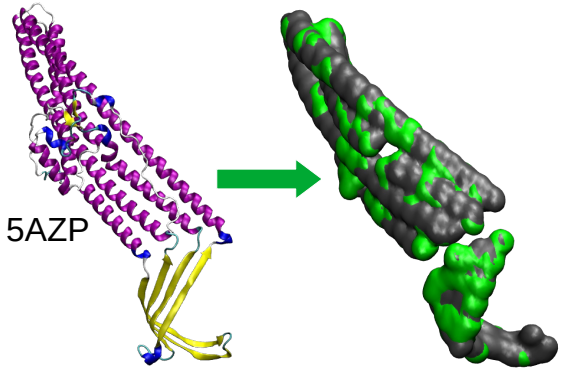

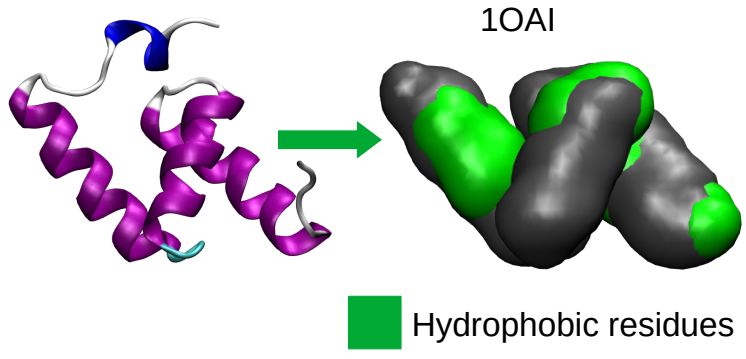

Hydrophobic residues

α-synuclein fonction and pathology

Li A, Rastegar C, Mao X. α-Synuclein Conformational Plasticity: Physiologic States, Pathologic Strains, and Biotechnological Applications. Biomolecules. 2022 Jul 17;12(7):994.

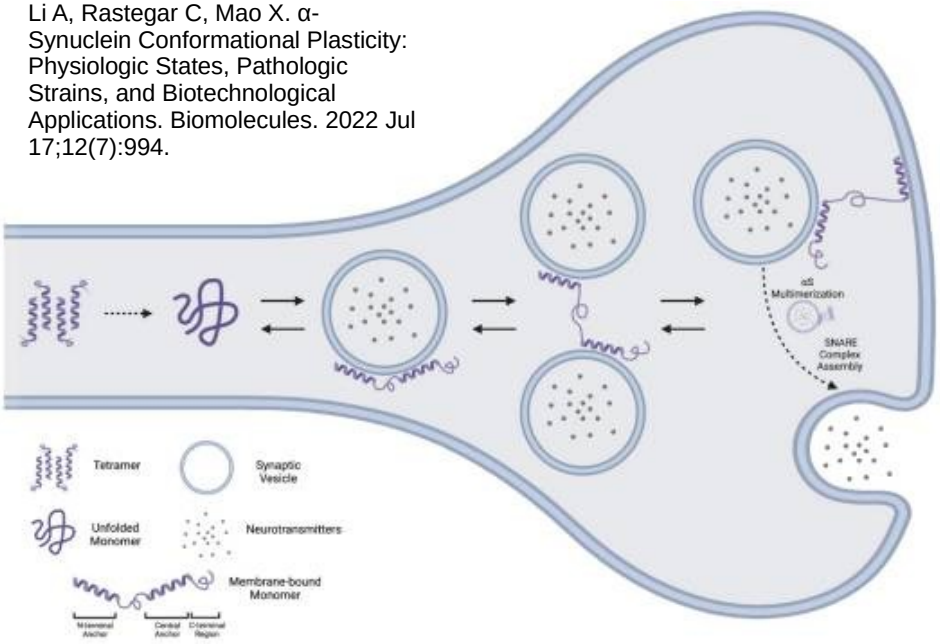

1XQ8

Ulmer TS, Bax A, Cole NB, Nussbaum RL. Structure and dynamics of micelle-bound human alpha-synuclein. J Biol Chem. 2005 Mar 11;280(10):9595-603.

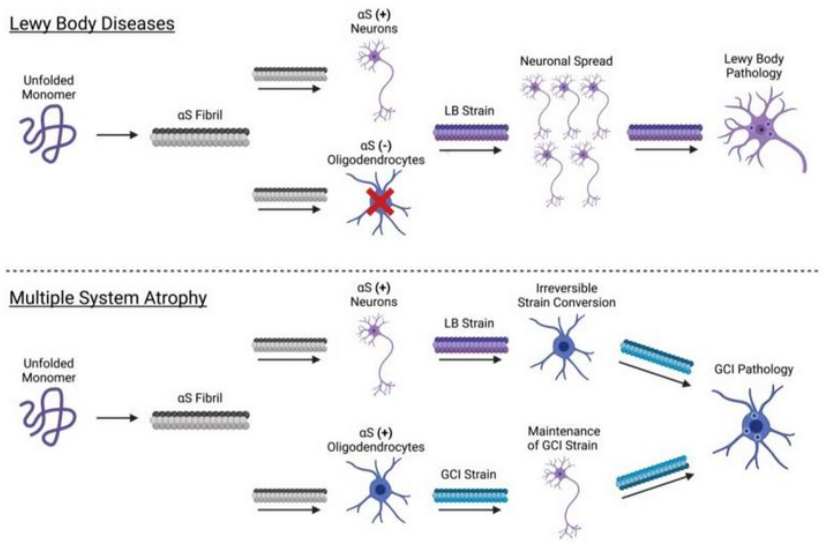

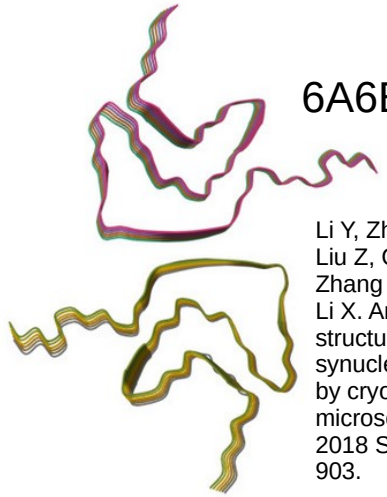

6A6B

Li Y, Zhao C, Luo F, Liu Z, Gui X, Luo Z, Zhang X, Li D, Liu C, Li X. Amyloid fibril structure of α-synuclein determined by cryo-electron microscopy. Cell Res. 2018 Sep;28(9):897-903.

α-synuclein fonction and pathology

α-Synclein monomers : synaptic vesicles cluster

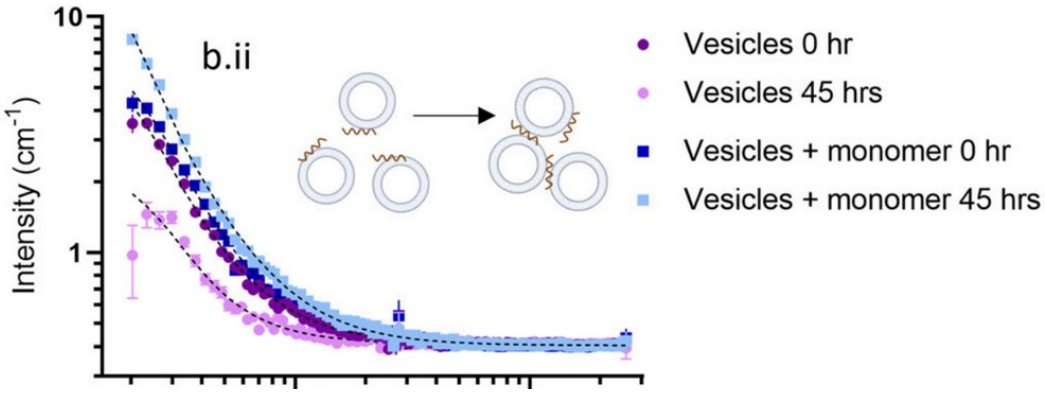

α-Synclein fibrils: synaptic vesicles desintegrate

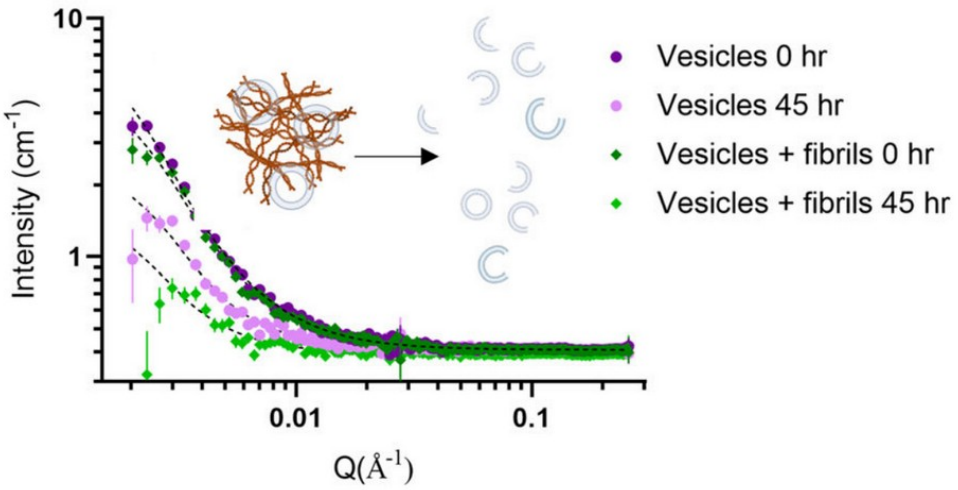

Stephens AD, Villegas AF, Chung CW, Vanderpoorten O, Pinotsi D, Mela I, Ward E, McCoy TM, Cubitt R, Routh AF, Kaminski CF, Kaminski Schierle GS. α-Synuclein fibril and synaptic vesicle interactions lead to vesicle destruction and increased lipid-associated fibril uptake into iPSC-derived neurons. Commun Biol. 2023 May 15;6(1):526Z

α-synuclein fonction and pathology

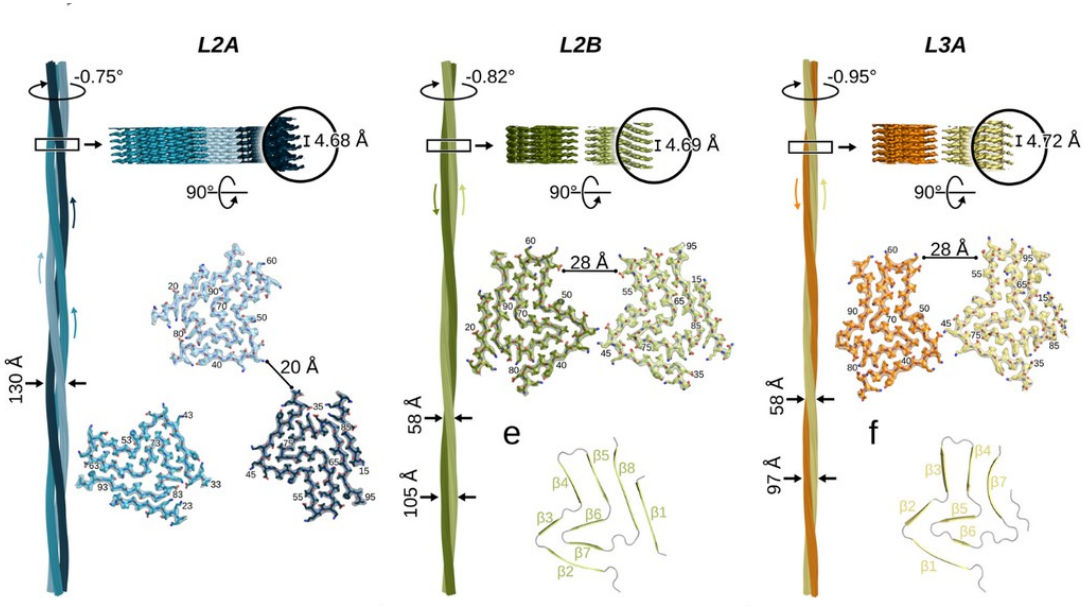

Cryo-EM structures

Acyl chains
Choline nitrogen
Phosphate
Sodium ions
Chloride ions

Molecular Dynamics simulations

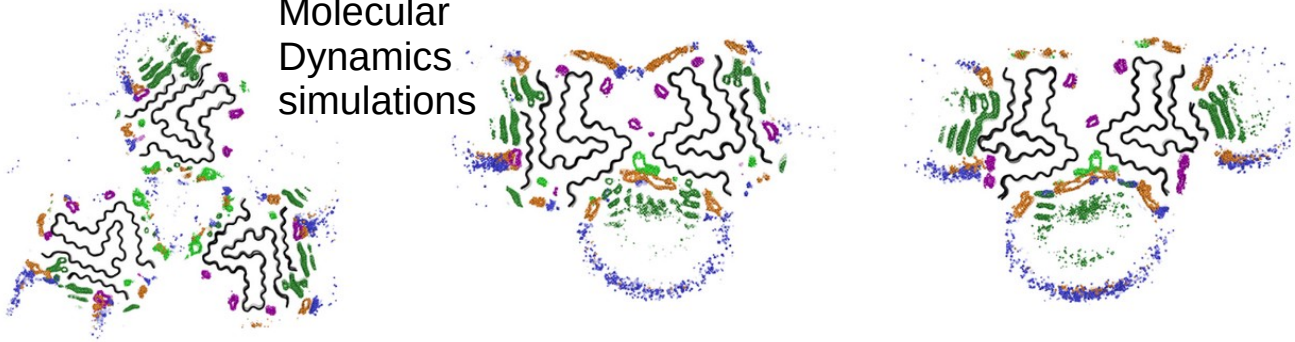

Frieg B, Antonschmidt L, Dienemann C, Geraets JA, Najbauer EE, Matthes D, de Groot BL, Andreas LB, Becker S, Griesinger C, Schröder GF. The 3D structure of lipidic fibrils of α-synuclein. Nat Commun. 2022 Nov 10;13(1):6810.

Towards the modeling of a fibril

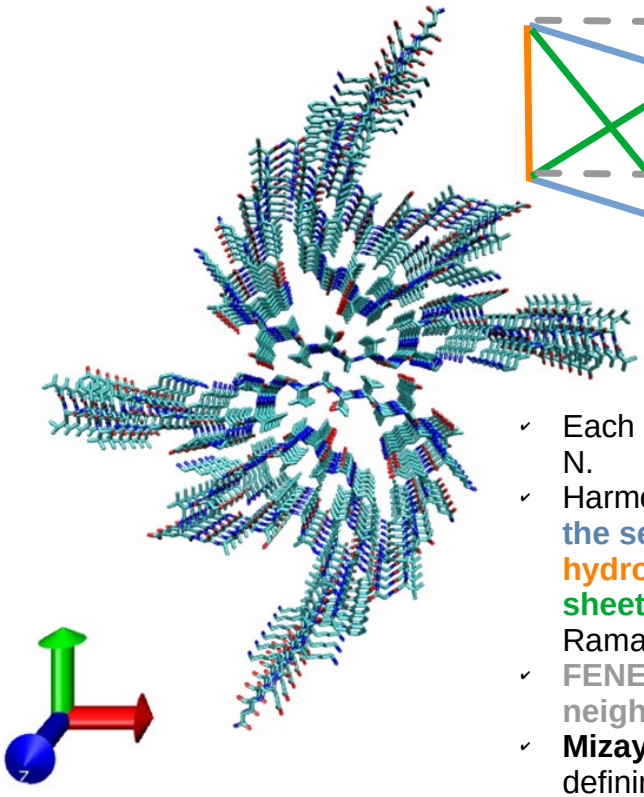

PDB 6A6B

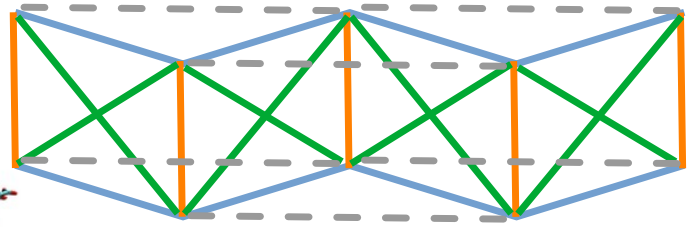

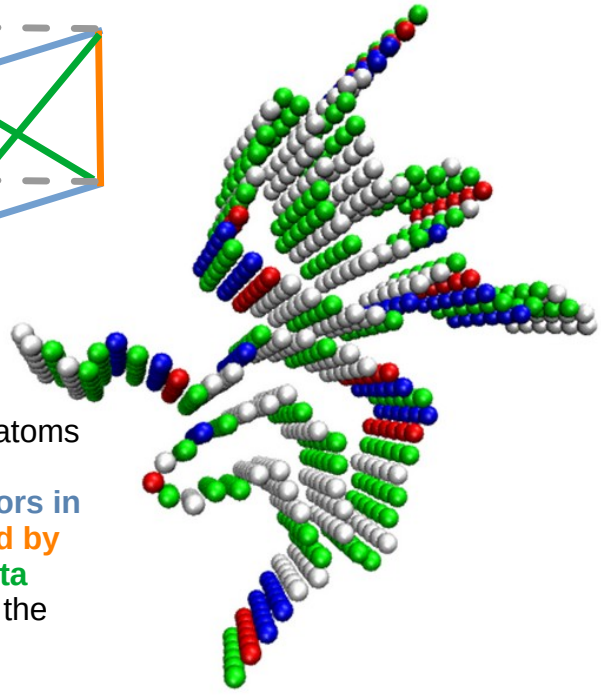

- Each bead at the position of nitrogen atoms N.
- Harmonic springs **between N neighbors in the sequence**, **between N connected by hydrogen bonds** and **to keep the beta sheet planarity** in order to reproduce the Raman spectrum of an amyloid fibrils.
- **FENE interaction between second neighbor's beads**
- **Mizayawa-Jerningan contact energies** defining the depth of Lennard-Jones– between beads,according to the type of amino-acid.

Lorène Schad (M2) and Martin Michael Müller, work in progress

Towards the modeling of a fibril

Conformational drift and internal dynamics

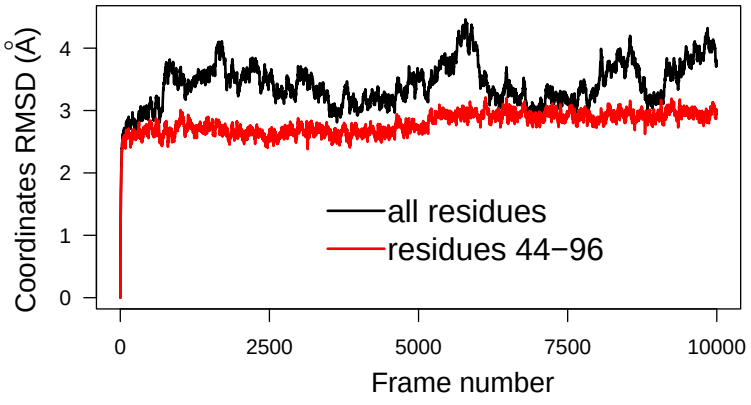

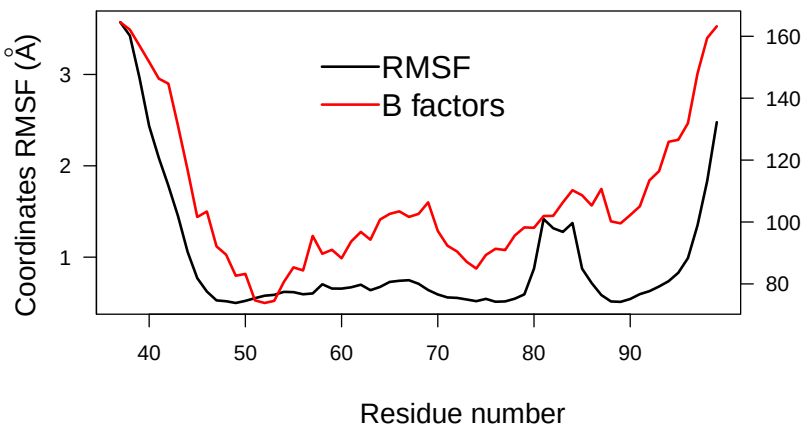

Relative orientation of the two β-sheets

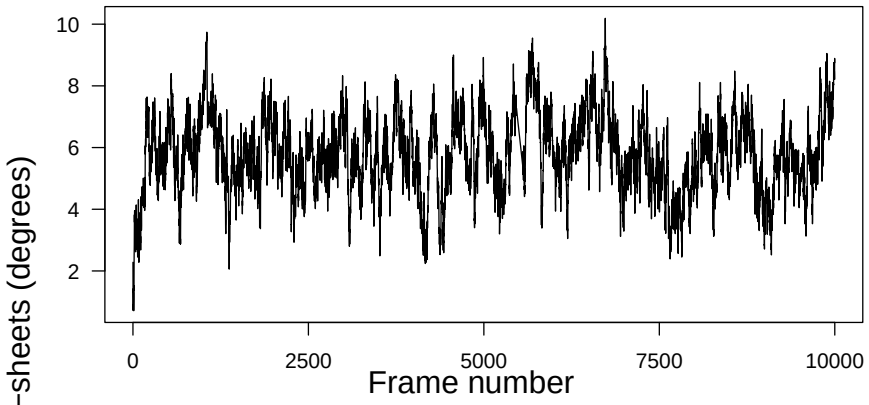

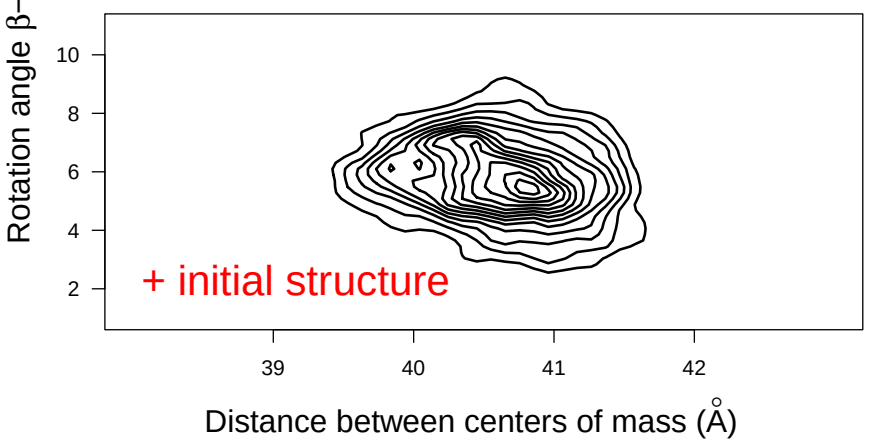

Lorène Schad (M2) and Martin Michael Müller, work in progress

Acknowledgements

Martin Michael Müller
Université de Lorraine
LPCT, Metz

Marina Botnari, PhD (2024-)
Alessandro Presutto, PhD (2025-)
Alexandre Delort
Jordan Klein (M2)
Lorène Schad (M2)

multiBioStruct PRCI ANR-MOST
anr.fr/Project-ANR-19-CE45-0019

Antonio Mucherino
IRISA

Leo Liberti
LIX, CNRS

Carlile Lavor
UNICAMP

Chi-Fon Chang
Academia Sinica

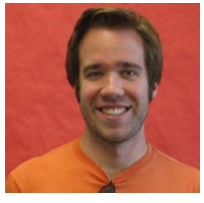

Bradley Worley
Scientist Atomwise

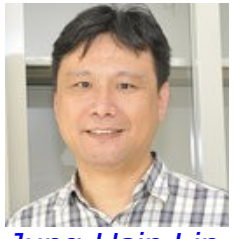

Jung-Hsin Lin
Academia Sinica

ShuYu Huang
Academia Sinica

Orion Shih *U-Ser Jeng*
NSRRC